EVALUATING THE EFFICACY OF RADIATIVE DRY SANITATION TECHNIQUES ON SALMONELLA-INOCULATED STAINLESS STEEL SURFACES POST VISIBLE CLEANING

By

Kasey L. Nelson

A THESIS

Submitted to
Michigan State University
in partial fulfillment of the requirements
for the degree of

Biosystems Engineering – Master of Science

2024

ABSTRACT

Salmonella cross-contamination in flour production facilities remains a recalcitrant problem, requiring effective low-moisture cleaning and sanitation. For research on this topic to be effective, dry inoculation methods must accurately model the powder accrual and the transfer of *Salmonella* from flour to equipment surfaces. Additionally, radiative sanitation technologies could provide quick and effective surface sanitation, given a sufficient intensity. Therefore, it is necessary to understand the relationship between radiation dosage and *Salmonella* reduction on stainless-steel (SS) surfaces. The objectives of this research were to (1) develop a replicable methodology employing electrostatic powder coating technology to apply inoculated, fabricated all-purpose flour onto SS surfaces, (2) generate the efficacy data for radiative dry sanitation technologies (UV-C, Far UV-C, and Infrared) achieving minimum 3 log reduction of *Salmonella* (log CFU/cm^2), and (3) develop surface inactivation models for the *Salmonella* on visibly clean SS surfaces in low-moisture environments. All-purpose wheat flour was fabricated and inoculated with a 6-strain *Salmonella* cocktail. The inoculated flour was adhered to #304 and #316 grade SS using an electrostatic powder coating apparatus. Subsequently, the SS was cleaned with a brush until visibly clean and then exposed to UV-C, Far UV-C, and IR radiation. Thereafter, the surface inactivation models were developed based on the log population counts remaining on SS surfaces and the total energy deposited as a function of the applied radiation intensity and the duration of radiation exposure. The dry powder coating inoculation methodology proved to be consistent and replicable at pilot scale, achieving ~4 log CFU/cm^2 on the surface of #304 brushed finish and #316L brushed finish SS coupons. Furthermore, this study demonstrated the potential application of UV-C and IR technologies for dry sanitation on visually clean, stainless steel surfaces across various grades and finishes.

ACKNOWLEDGEMENTS

My sincerest thanks to Dr. Sanghyup Jeong, my major advisor. His ability to distill complex engineering problems that seem impossible to solve into actionable tasks that further scientific understanding toward current issues in food production cannot be overstated. His guidance, advice, and patience helped me overcome many roadblocks to my success.

I also greatly appreciate my committee members, Dr. Bradley Marks, and Dr. Teresa Bergholz. I would not have been able to succeed without their collective expertise and insight, especially with their limited and highly valuable time.

Next, thank you to the Food Safety Engineering Laboratory staff, specifically Michael James and Dr. Ian Hildebrandt, for their assistance with a large amount of small things: equipment, troubleshooting, best laboratory and modeling practices, and answering minor but important questions. Additionally, thank you to Phil Hill for fabricating components of my experimental equipment.

Thank you to my fellow graduate students and undergraduate coworkers. My work would not have been feasible without their support. Thank you to Ian Klug for his eagerness to help with experimentation, his innumerable hours of help, and company. Thank you to my family and friends, who cheered me on from near and far, and to the Nokomis Cultural Heritage Center, which was a source of community and generational knowledge throughout the course of my degree.

And finally, thank you to Nicole Hall, whose single suggestion to research the microbial safety of flour during a team meeting in my sophomore year changed the course of my academic career.

Chi-miigwech to you all for your support.

This work is supported by the Agriculture and Food Research Initiative, Sustainable Agricultural Systems Program grant no. 2020-680-31822 from the USDA National Institute of Food and Agriculture. Any opinions, findings, conclusions, or recommendations expressed in this publication are those of the author(s) and do not necessarily reflect the view of the U.S. Department of Agriculture.

TABLE OF CONTENTS

LIST OF TABLES

LIST OF FIGURES

INTRODUCTION

Problem Statement

Recent outbreaks and recalls of low-moisture food products such as flour have been linked to *Salmonella*, raising significant public health concern. Ensuring cleanliness and sanitation in low-moisture food production is critical for maintaining product safety and protecting public health. Challenges in these low-moisture environments include the need to limit water usage in the cleaning and sanitation processes to prevent the outgrowth of pathogens, yeasts, and molds. The prohibition of water as a sanitation compound carrier in dry environments necessitates alternative, more labor-intensive cleaning and sanitation approaches to meet similar sanitation efficacies to other industry sectors.

Significant knowledge gaps exist in research related to dry sanitation, particularly regarding ideal food contact surface inoculation strategies, the application of efficacious and practical dry sanitation technologies, and the generation of sanitation parameters for future reference.

To mimic potential contamination in dry processing environments, a dry inoculation methodology is essential. This method must use minimal moisture and reflect the realities of powder accrual on equipment surfaces during production. Food-grade stainless steel is a commonly used surface in food production environments, and characteristics such as chemical composition (grade) and the surface finish can affect the survival of adherent bacterial populations. An ideal inoculation method would leave detectable bacterial populations on the surface after cleaning, enabling the assessment of the effectiveness of dry sanitation technologies.

Although several proof-of-concept studies have explored non-aqueous sanitation technologies, such as electromagnetic radiation for low-moisture foods and food contact surfaces, many lack consistent, crucial data needed for industrial application, including radiation intensity, the distance from the emitter to the target surface, and the inactivation models on the target surface.

Goals and Objectives

The objectives of this experiment were to:

1. Develop a replicable and consistent electrostatic powder coating dry inoculation methodology that can achieve *Salmonella* populations (> 4 log CFU/cm^2) on stainless steel surfaces after brushing to "visibly clean."
2. Generate the efficacy data for several radiative, non-aqueous sanitation technologies (UV-C 254 nm, Far UV-C 222 nm, Infrared) on visibly clean stainless steel surfaces achieving minimum 3 log reduction of *Salmonella* (log CFU/cm^2) by varying the total energy deposited.
3. Develop surface inactivation models for *Salmonella* on stainless steel surfaces for each radiative sanitation technology in low-moisture food production environments.

LITERATURE REVIEW

Recent Outbreaks of *Salmonella* Linked to Flour Products

Foodborne pathogens in low-moisture foods (LMFs) pose significant concerns for food manufacturers, public health agencies, and consumers. The rise in outbreaks and recalls related to low-moisture foods has heightened public awareness of the risks associated with their consumption.

In the United States, numerous recalls have involved *Salmonella* contamination in flour and wheat-containing products. In 2008, a salmonellosis outbreak was linked to *S.* Agona occurred in wheat and rice cereal (Centers for Disease Control and Prevention, 2008), and within the same year, a New Zealand-based *Salmonella* Typhimurium phage type 42 outbreak was linked to consumption of contaminated raw flour (McCallum et al., 2013). In 2018, *S.* Mbandaka was found in cereal, which was subsequently recalled. Most recently, in 2023, recalls of all-purpose flour (Centers for Disease Control and Prevention, 2023a), and raw chocolate chip cookie dough (Centers for Disease Control and Prevention, 2023b) were linked to *S.* Infantis and *S.* Enteritidis, respectively.

Additionally, previous outbreaks linked to other low-moisture foods include a 1998 outbreak of *S.* Agona in toasted oats cereal (Centers for Disease Control and Prevention, 1998), a 2003 outbreak of *S.* Enteritidis PT 30 in almonds (Centers for Disease Control and Prevention, 2004), a 2007 outbreak of *S.* Tennessee in peanut butter (Centers for Disease Control and Prevention, 2007), a 2009 outbreak of *S.* Montevideo outbreak in black and red pepper (Centers for Disease Control and Prevention, 2010), and a 2013 outbreak of *S.* Mbandaka in tahini (Centers for Disease Control and Prevention, 2013).

The recurrent outbreaks of *Salmonella*, including those in low-moisture foods such as cereals and flours, underscore its critical importance in food safety protocols, highlighting the need for stringent contamination prevention measures across diverse food products.

Salmonella

Salmonella is a Gram-negative, rod-shaped enteric bacteria. They can be classified into typhoidal and non-typhoidal strains, each causing different health effects and outcomes for those infected. The most common infectious serovars in the United States are *S.* Enteritidis*, S.* Newport, and *S.* Typhimurium (Centers for Disease Control and Prevention, 2016).

Certain strains of *Salmonella* (Typhi, Paratyphi A, B, and C) can cause life-threatening illnesses when present in the host's bloodstream. Typhoidal strains of *Salmonella* can only be shared between humans (Bennett, 2020), usually through a fecal-oral route. Typhoidal strains are associated with typhoid fever, which typically presents as a severe, lengthy fever in conjunction with headache, constipation, or diarrhea (CDC Yellow Book, 2024b). Without medical treatment, serious complications may arise, including gastrointestinal hemorrhage. Untreated cases may last up to a month and can have a fatality rate of 10–30% (CDC Yellow Book, 2024b).

Non-typhoidal strains have multiple reservoirs for transmission to human hosts, whether they be zoonotic or environmentally based. Common sources include domestic animals, raw food products, or contaminated water sources (CDC Yellow Book, 2024a). Non-typhoidal salmonellosis typically present with severe diarrhea, fever, heavy abdominal cramping, and loss of appetite.

As of 2011, 1.2 million cases of non-typhoidal *Salmonella* occurred annually in the United States (Scallan et al., 2011). The considerable burden of illness has significant impacts on public health.

Unique Challenges: *Salmonella* and Low-Moisture Foods

Low-moisture foods, which have a water activity (a_w) below 0.86, lack the environmental and physical characteristics that typically support the survival of foodborne microbes. The lower the water activity for a food product, the less water is available for pathogen use, serving as a barrier to pathogen growth. Particularly, some strains of *Salmonella* can express resistance to processing steps such as drying and thermal treatment due to their thermal and desiccation resistance (Liu et al., 2018; Smith, et al., 2016). Some examples include *Salmonella* Enteritidis PT 30 (ATCC BAA-1045), known for its thermal resistance and linked to almond outbreaks from 2003–2004 (Centers for Disease Control and Prevention, 2004), and *Salmonella* Reading (Moff 180418), which demonstrates both thermal and desiccation resistance in low-moisture food powders (Wei et al., 2020).

Prevalence and Viability of *Salmonella* in the Flour Milling Process

To understand how *Salmonella* accrues in milling end-products, field studies have been conducted to survey the microbiological backgrounds of incoming wheat from across the globe as a point of entry into the milling process.

A 2003 Australian study by Berghofer, et al. surveyed nine mills owned by three companies, conducting APC counts, total coliform counts, spores, and yeast tests to determine the microbiological background of wheat within Australia (n=650). The study found minimal populations of *E. coli* and *Salmonella*, with no pathogenic *Salmonella* serovars found in the samples, although two strains of environmental *Salmonella* were isolated. Notably, most wheat contaminants were present on the outer layers of the grain (i.e., wheat bran and germ) (Berghofer et al., 2003). The study also highlighted early discussions on product recontamination via milling equipment.

Additional microbiological surveys of wheat, corn, oats, whole wheat, and durum were taken from 2003–2005 in research by Sperber (2007). After sampling wheat from 2003–2005 (*n*=4,358), the study found a low prevalence of *Salmonella* (0.14%) in tested samples.

Later research by Sabillón, et. al, investigated the varying microbial load of hard red winter wheat produced in the midwestern United States (Sabillón et al., 2016). Three different lines of hard red winter wheat were grown in separate locations and exposed to different environmental conditions over two growing seasons. Like Berghofer, et al., the wheat samples (*n=81*) were tested for microbes and fungus related toxins using APC, yeasts, molds, and coliform bacteria tests. Samples selected for *Salmonella* testing were enriched using buffered peptone water and transferred into tetrathionate broth, a selective medium. The study did not detect the presence of *Salmonella* or *E. coli* in any samples. Importantly, the microbial load of wheat varied depending on growth location, with environmental factors like seasonality, relative humidity, and rainfall further impacting microbial load. More research was needed to characterize the microbial load of wheat for large sample sizes to better reflect the large scale, multi-seasonal, and continuous nature of wheat processing.

Lastly, Myoda, et al. conducted a three-year study that sampled wheat prior to entering the milling process (*n*=5,176) (Myoda et al., 2019). Wheat samples, including hard red spring, hard red winter, soft red winter early, and soft red winter late, were tested for *E. coli* and *Salmonella*, with 3,891 of the samples tested and 1.23% of testing positive for *Salmonella* (0.110 ± 0.448 MPN/g, ~41 MPN per 375 g sample) (Myoda et al., 2019).

Overall, the microbiological surveys highlighted a low prevalence of *Salmonella* and other foodborne pathogens in wheat products, a finding that contrasts with the rising number of outbreaks and recalls.

Fate of *Salmonella* During Flour Processing and Post-Processing

Given the reported low prevalence of *Salmonella* in incoming wheat, one might wonder why are extra populations are measured in milling end products. Factors influencing the survival of *Salmonella* in flour, such as fluctuations in relative humidity within the processing system, shifts in the water activity of products, and cross-contamination from soiled equipment, explain this necessity.

Generally, the flour milling process reduces water usage to inhibit the growth of pathogens, molds, and yeasts. During tempering, a step in the milling process, a minute amount x of water (1–3% of the wheat berry mass) is used to bring the wheat berries to their optimal moisture content before milling, although the total added amount of water can vary due to several factors including initial moisture content (Posner & Hibbs, 2005). This step may seem counter-intuitive to prevent the growth of unwanted microbes. Notably, a study by Lin, et. al, found that significant increases in wheat grain a_w during the tempering process did not significantly increase native microbes (mesophiles and coliforms) or intentionally added pathogen populations (2023).

Nonetheless, research by Sperber and the North American Millers' Association emphasized the importance of limiting water use beyond tempering: the addition of moisture to products can cause growth of pathogens, molds, and yeasts once the a_w is greater than 0.85 (Sperber & North American Millers' Association, 2007). The fluctuation of water activity inside the products during processing can also have a detrimental effect on product safety. Carter, et. al determined that tempered wheat held at $a_w > 0.70$ for over 24 h could cause unwanted mold growth on wheat berries (Carter et al., 2015). Therefore, monitoring the relative humidity and

moisture content of the wheat and the production environment is an important consideration for product quality and safety.

This observation of minimized water use contrasts sharply with the sanitation methods prevalent in other industries, where aqueous sanitizers are widely used, especially in clean-in-place operations for dairy and juice processing. In low-moisture environments, water cannot serve as a carrier fluid for chemical compounds to inactivate pathogen, mold, and yeast, making equipment sanitizing challenging. Additionally, moisture introduced during the sanitation could affect the quality and safety of subsequent products.

Even with the strict control of moisture, *Salmonella* and other pathogens can contaminate equipment with low levels in a viable state. Research by Kusumaningrum, et. al found that *S.* Enteritidis*,* when allowed to contaminate surfaces at high levels (7 log CFU/100 cm^2) was detected on #304 stainless steel after 96 hours post-contamination (Kusumaningrum et al., 2003). At moderate levels (5 log CFU/cm^2), *S.* Enteritidis was detectable until 24 hours passed. Although 24 hours is a relatively short period, residual populations on stainless steel surfaces within the processing line can cross-contaminate the next batch of flour.

A later study in 2021 by Sabillón et al., investigated the prevalence of generic *E. coli* on relevant equipment surfaces in a flour mill. . Milling equipment was swabbed to enumerate any potential *E. coli,* coliforms, yeasts, and molds remaining on equipment surfaces from incoming wheat grain to flour packaging. Quantifiable amounts of *Enterobacteriaceae* (2.3 ± 1.0 log CFU/cm^2) were found within the inside walls of the flour grinding machines. In comparison, the flour handling and storage equipment had 1.1 ± 1.6 log CFU/cm^2, specifically within the finished flour mixer (Sabillón et al., 2021).

After production, flour is often stored for extended periods before consumption. The survival rates of heat and desiccation-resistant *Salmonella* strains in low moisture foods post-production has been previously studied (Syamaladevi et al., 2016; Villa-Rojas et al., 2017; Xu et al., 2019). Thus, recurring consumption of the contaminated product could cause multiple occurrences of illness, emphasizing the importance of sanitation during and after production in low moisture food environments.

Sanitation In Low-Moisture Environments

Current practices for sanitation in low-moisture food processing environments use multiple techniques and tools to inactivate microorganisms on equipment after cleaning, the physical removal of debris. One standard technique is the use of non-aqueous chemical sanitizers which can be applied directly to food contact surfaces to inactivate microbes. Although effective, some non-aqueous sanitizers include water as part of their formulation, introducing undesirable moisture into the processing environment. Harada & Nasciemento found that a quaternary ammonium compound +isopropyl alcohol solution (specifically, didecyldimethylammonium chloride (0.015% v/v), sequester, isopropyl alcohol (25% v/v) and water) inactivated pathogens on stainless steel and polypropylene, albeit with a “weak performance” (Harada & Nascimento, 2021) in comparison to the other dry sanitation technologies used within the study.

While “non-aqueous” sanitizers are not the ideal method for dry sanitation, they are employed in some food production environments such as almond processing (Du et al., 2010) due to a lack of feasible alternatives, especially since the solution can flow into cracks and crevices (Kane et al., 2016). The preferred dry-sanitation method should be non-aqueous, safe for both the product and personnel, cost-effective, and require short exposure times for treatment efficacy. Two potential non-aqueous technologies that could be used alongside non-aqueous

sanitizers, ultraviolet-C (UV-C) radiation and infrared radiation (IR), utilize different wavelengths of electromagnetic radiation to inactivate pathogens.

Overview of Electromagnetic Radiation

There are two main models of classifying electromagnetic radiation: the classical model and the quantum model. The classic model describes the oscillations of electric and magnetic fields by interactions between charged particles (Zhabinskaya & University of California Davis, 2023a). The quantum model describes the excitation of photons to different quanta. The higher the quanta, the higher the frequency of the particle, hence the higher radiative energy the particle can possess (Zhabinskaya & University of California Davis, 2023b). The dual nature of electromagnetic radiation being both an electromagnetic wave and a particle allows for a range of applications toward pathogen control in different food products and food contact surfaces.

Given enough energy, select wavelength bands of electromagnetic radiation (X-ray and gamma) can promote ionization, where an atom gains or loses electrons within atomic valence shells through collisions with energetic particles. Ionizing radiation can effectively inactivate microbes in a variety of mediums by removing electrons from biological molecules that are crucial for survival. However, this phenomena poses a significant risk to human health. Alternatively, non-ionizing, lower energy radiation sources such as infrared and ultraviolet can effectively inactivate microbes in food processing environments.

Infrared Radiation. Infrared radiation is a form of electromagnetic radiation between 700–1000 nm that is invisible to the human eye. The inactivation principle involves heating the target microorganism until it can no longer function. Molecules within the microorganism absorb IR, causing vibrations that increase the temperature of the cell. Bacteria, including *Salmonella,* can be thermally inactivated in both normal or desiccated states (Xu et al., 2020).

IR can penetrate thin surfaces and access hard-to-reach cracks and crevices on surfaces and equipment that are normally inaccessible to tools and hands. IR can be generated using various sources such as heat lamps, ceramic and metal shielded heat coils, and quartz halogen tubes. Key considerations for implementing IR include the housing materials, IR absorption, the distance between target surface or product and the IR emitter, and duration of exposure.

Ultraviolet Radiation. Ultraviolet radiation (UV) is a form of electromagnetic radiation with a frequency above visible light, having shorter wavelength than both IR and visible light. UV can be further classified into three main wavelength bands: UV-C (100–280 nm), UV-B (280–315 nm), and UV-A (315–400 nm) (International Organization for Standardization, 2007).

Ultraviolet radiation uses shorter, more powerful wavelengths in comparison to infrared radiation. UV-C rays specifically provide ionizing energy to break bonds within DNA and RNA molecules toward the inactivation of microorganisms.

Exposure to UV-C radiation leads to the dimerization of the pyrimidine bases (thymine, uracil, and cytosine) in eukaryotes, prokaryotes, and viruses. Dimerization occurs when the double carbon bond between thymine and cytosine (or uracil) absorbs UV-C radiation and severs (Goodsell, 2001). The severed bond can reattach to the next base on the same DNA strand and has several notable variations in chemical structure (Batista et al., 2009; Napoleao et al., 2023). Dimerized DNA and RNA bonds are mutagenic and cannot be used for normal genetic replication, protein synthesis and other cellular functions. Nucleic acids are especially susceptible to UV-C wavelengths within the 200–300 nm range (Beck et al., 2016; Hessling et al., 2021). UV-C radiation effectively inactivates bacteria, fungi, and viruses on various products and surfaces, requiring specific wavelengths and UV-C dosages tailored to the critical inactivation parameters of the target microorganism.

UV-C can be generated by mercury lamps, light emitting diodes (LEDs), excimer lamps, or pulsed xenon lamps. Common low-pressure mercury bulbs emit UV-C at 254 nm, which are often used within UV-C disinfection systems and have a wide array of data available for dosage experiments (Giese & Darby, 2000). LED lamps can be modified to emit UV-C between 200–280 nm. Excimer lamps emit UV-C at 222 nm. Pulsed xenon lamps have a wide range of emitted radiation (200–1000 nm) but require filtering of the emitted waves to meet a target wavelength (Demeersseman et al., 2023).

Safety of UV-C Generating Devices

UV-C can cause damage to human skin and eyes, including facial erythema (skin reddening) and photokeratitis ("snow-blindness") (Ramos et al., 2020; Sliney, 2013). UV-C emitted at 254 nm has been found to alter oxidative stress and inflammatory response pathways on reconstructed human skin models in comparison to 222 nm, a lower, Far UV-C wavelength (Napoleão et al., 2023).

Recent research has indicated that Far UV-C has a reduced risk of skin and eye damage in comparison to 254 nm UV-C. A study by Buonanno, et al. claimed that 222 nm UV-C "produces almost no premutagenic UV-associated DNA lesions in a 3D human skin model and it is not cytotoxic to exposed mammalian skin" (2017). The study also achieved ~3 log reduction of methicillin-resistant *Staphylococcus aureus* using Far UV-C at a UV fluence of ~15 mJ/cm^2 (Buonanno et al., 2017). Additional research by Kaidzu, et al., found that Far UV-C radiation did not penetrate beyond the corneal limbus, the border between the cornea and white of the eye, in rat and porcine corneas (2022). However, 254 nm penetrated to the basal cell layer where corneal limbus cell replication occurs and exhibited signs of DNA dimerization (Kaidzu et al., 2022).

Far UV-C has been used in hospital settings, which are similar to dry processing environments due to the frequent sanitation of surfaces to prevent cross-contamination and disease. A 2023 study by Navarathna, et al. used a filtered 222 nm Far UV-C device in comparison to sodium hypochlorite disinfectant wipes on non-porous, high-touch surfaces, including bedrails, tables, and workstations (n=86). The UV-C device was positioned 2.54 cm from each target surface (confirmed with a built-in indicator) and emitted UV-C for 30 s with an intensity of ~3.6 mW/cm^2. The contact surfaces for the UV-C device had a mean 22.2 CFU per 25 cm^2 pre-treatment and had an 81.4% reduction in surface populations (~4.1 CFU) post-treatment (Navarathna et al., 2023). The device was suggested for use when manual disinfection is infeasible or as a substitute for moderate disinfection capabilities.

If UV-C generating devices at lower wavelengths can inactivate pathogens with comparable population reductions and intensities such as UV-C 254 nm, Far UV-C devices may pose as a “safer alternative” for sanitation personnel when applied to low-moisture food contact surfaces.

Applications of UV-C and IR for Low-Moisture Food Safety

Although research on UV-C and IR based sanitation methods for low-moisture foods and their contact surfaces is limited, notable studies exist.

A 2011 study by Hamanaka, et al., studied the effects of synergistic UV and IR radiation on *Rhodotorula mucilaginosa,* a yeast that can impact fig fruits, using UV-C (253.7 nm) and IR (950 nm) sources. The findings showed that UV-C and IR had different levels of efficacy (Hamanaka et al., 2011). Specifically, IR treatment resulted in a 1 log reduction of *Rhodotorula mucilaginosa* on fig surfaces within 30 seconds (Hamanaka et al., 2011), whereas UV-C treatment achieved a 2.5 log reduction in the same duration. Remarkably, a 3 log reduction in

populations occurred after a sequential 30 second dose of IR followed by UV-C (Hamanaka et al., 2011).

Another study by Ha & Kang investigated the effect of UV-C and IR on red pepper powder inoculated with *S.* Typhimurium and *E. coli* O157:H7. The study achieved a 3.34 log reduction in *Salmonella* populations within red pepper powder samples after 5 min of concurrent IR and UV-C exposure (Ha & Kang, 2013).

A 2021 study by El Darra, et al. measured the effects of IR, UV, and ozone on dried onion flakes and black pepper. The study used a 100 W IR bulb, a 4 W UV-C lamp, and a 25 W ozone purifier to inactivate *E. coli* on the samples in a custom-made decontamination system. After a sequential treatment of ozone for 2.5 min followed by concurrent UV and IR for ten min, black pepper samples received a 4.20 log reduction in *E.* coli populations, a higher kill than the technologies being used sequentially (El Darra et al., 2021). The study showed the potential for further work using the synergistic effects of UV-C and IR in low-moisture foods.

An in-depth study by Nyhan, et. al, investigated the efficacy of different UV-C inactivation technologies within inoculated low-moisture food powders (onion powder, cheese and onion powder, chili powder, and garlic powder) with additional observations on plastic surfaces. UV-C lamps and UV-C LEDs, each at different wavelengths, were used to inactivate *L. monocytogenes, E. coli, B. subtilis, and S.* Typhimurium in the target products. The study used a wide range of UV-C wavelengths, from 254 nm, 270 nm, to 365 nm to examine potential differences in efficacy. There were significant differences in efficacy depending on the food product, UV-C device, and applied wavelength. *S.* Typhimurium had over a 4 log CFU reduction in populations after a five second treatment using a 270 nm UV-C LED mounted 2 cm from the target surface (Nyhan et al., 2021). This study had the highest reduction with the shortest time in

comparison to other literature, likely due to the minimized distance between the UV-C LED emitters, the target surface, and selected low-moisture food powders.

Applications of UV-C and IR Toward Low-Moisture Food Contact Surfaces

Most of the research on food contact surface sanitation experiments involves food-grade stainless steel (SS), which is commonly used in food manufacturing equipment.

Research by Gabriel et. al, used UV-C and cold atmospheric plasma on stainless steel to inactivate *S. enterica*. The study determined the time for a 2 log reduction on the surface of #304 stainless steel with a 2B finish to be 462.56 ± 560.15 s (mean ± SD), approximately 7.7 min (Gabriel et al., 2018). Harada and Nasciemento also studied multiple dry sanitation methods on stainless steel, along with polypropylene. UV-C, dry heat, ozone, and non-aqueous sanitizers were used to inactivate *Listeria monocytogenes* biofilms. After generating a Weibull model to characterize the various methods of inactivation, it was found that UV-C required 390 min of exposure to achieve a 5 log reduction in populations on stainless steel, while dry heat required 170 min. The time for a 5 log reduction decreased significantly for polypropylene, requiring only 6.1 min for UV-C and 54 min for dry heat (Harada & Nascimento, 2021).

A compilation of studies using UV-C and IR in low moisture foods and food contact surfaces is featured in Table 1.

Table 1: Survey of studies utilizing UV-C and IR in low-moisture food sanitation experimentation

Citation	Food product / surface	Pathogens of interest	Technologies	Treatment Parameters					
				Wattage	Wavelength (if applicable)	Intensity of radiation	Length of exposure	Distance from surface	Achieved log reductions
(Ha & Kang, 2013)	Red pepper powder	*E.coli O157:H7, S.* Typhimurium	Near infrared (Quartz halogen infrared heating lamp), UV germicidal lamp	NIR: 500 W	Not specified	2.62 mW/cm^2	0-5 min	Not specified	NIR-UV: 3.34 (5 min, *Salmonella*) synergistic
(Bozkurt & Uslu, 2022)	Petri dishes	*Staphylococcus aureus, Bacillus cereus, E. coli, Klebsiella pneumoniae*	Philips UV-C TUV PL-L 36W / 4P Germicidal light bulb	12.2 W	262 nm	Not specified	10 s, 20 s, 30 s, 45 s, 1 min, 2 min, 4 min, 10 min	24 cm	UV: 45s (17.95 CFU/mL, log 5.74), 30s (19.50 CFU/mL, log 5.70), 20s, (30 CFU/mL, log 5.52), and 10s (241.04 CFU/mL)
(Hamanaka et al., 2011)	Fig fruit, yeast cells	*Rhodotorula mucilaginosa*	WASAKI Electric Co. Ltd (IR + UV lamps)	Not specified	IR: 950 nm UV: 253.7 nm	IR: 14.8 mW/cm^2/nm UV: 31.7 mW/cm^2	15 s, 30 s, + combinations for each technology	8 cm (fruit), 13 cm (petri dish)	IR: 1 log (30 s), UV: 2.5 log (30 s), IR-UV: 3 log (30 s sequential)
(El Darra et al., 2021)	Dried onion flakes, black pepper	*E. coli*	IR lamp, UV lamp, ozone	IR: 100 W UV: 4 W	UV: 254 nm	Not specified	0–30 min (5 min intervals)	Not specified	Sequential IR and UV: ~4 log (2.5 min)

Table 1 (cont'd)

(Kim et al., 2023)	Black peppercorn	*S.* Typhimurium	Vacuum ultraviolet, Near-infrared radiation	IR: 500 W VUV: 42 W	UV: 185, 254 nm	IR: 141.75 μW/cm^2/nm VUV: 4.7 mW/cm^2	5, 10, 15, 20 min	17 cm	Combined IR+UV: ~1.74 log (5 min)
(Nyhan et al., 2021)	onion powder, garlic powder, cheese and onion powder and chilli powder	*L. monocytogenes*, *S.* Typhimurium, *B. subtilis*	UV mercury lamps, UV-C-LEDs, and UVA-LEDs	50 W	UV: 254, 270, 365 nm	Not specified	5, 10, 20, 40 s	2 cm	~ 3.5 log (40 s, onion powder, *S.* Typhimurium)
(Ruiz-Hernandez et al., 2021)	Peanuts, almonds	*S.* Typhimurium	UV-C lamp	Not specified	254 nm	10 mW/cm^2	2.5–30 min	10 cm	2.39 log (30 min, almonds)
(Kim et al., 2016)	Sliced cheese	*E. coli*, *S.* Typhimurium, *L. monocytogenes*	UV-C LEDs, UV-C lamp	UV-C lamp: 16 W	266, 270, 275, 279 nm (LEDs), 254 nm (Lamp)	4–5 μW/cm^2	"Treatment times for the doses were calculated by dividing UV doses by intensities with an appropriate conversion factor."	4 cm	Not specified
(Gabriel et al., 2018)	Stainless steel	*Salmonella enterica*	UV-C lamp	15 W	~254 nm (253.97)	33.588 mW/in^2	0–180 s	9.8 cm	3.3 log (10 s, #304 SS 2B)
(Harada & Nascimento, 2021)	Polypropylene, stainless steel	*L. monocytogenes*	UV-C light	8 W	254 nm	6.5 mW/cm^2	0,5,10,15,30 min	15 cm	1.5 log (5 min)

Table 1 (cont'd)

(Bae & Lee, 2012)	Polypropylene, stainless steel	*S.* Typhimurium. *S. aureus*, *L. monocytogenes*	UV Sterilizer, model DS701	15 W	253.7 nm	0.24 mW/cm^2	30 min, 1, 2, 3 h	18 cm	3.06 log (3 h, stainless steel, *S.* Typhimurium)
(Yoon et al., 2018)	Pork, chicken, cabbage, milk, and distilled water transferred onto stainless steel and polypropylene	*E. coli*, *S.* Typhimurium, *L. monocytogenes*, *S. aureus*	UV Sterilizer, model DS701	15 W	253.7 nm	0.24 mW/cm^2	0, 30, 60, 120 min	~22 cm	~3.15 log (120 min, stainless steel, *S.* Typhimurium within chicken residues)

Importantly, some of the critical processing parameters used for radiative technologies featured in Table 1, such as the intensity of the emitted radiation, are not reported in all studies. The absence of these values obstructs practical comparisons between studies and the generation of dosage models.

Knowledge Gaps Within Current Literature: Dry Inoculation Methodologies

Current literature on cleaning and sanitation reveals knowledge gaps in the ideal inoculation methodology for simulating cross-contamination scenarios, and in determining the appropriate application parameters for dry sanitation techniques on low-moisture foods and food contact surfaces.

Modeling equipment surface contamination during low-moisture food processing can be achieved by directly inoculating the target food product. However, the chosen inoculation methodology can affect the survival rates of pathogens within the food matrix. Research by Hildebrandt, et. al emphasized how inoculation methodologies influence the behavior of *Salmonella* in low-moisture food products like flour (Hildebrandt et al., 2016). These methods simplify the experimental design, promote thermal and desiccation resistance of the selected strains, allow for analysis of worst case storage and thermal treatment scenarios in low-moisture foods, and improve experimental replicability. Yet, they do not accurately simulate potential contamination scenarios in dry processing environments. Additionally, certain liquid broth-based inoculation methods may inadvertently increase moisture level in the food product and the processing environment unless specific equilibration steps are followed post-inoculation.

Additional research into other inoculation methods such as biofilm formation for sanitation experimentation has been studied. A study involving *Listeria monocytogenes* biofilm formation on #304 SS surfaces adhered 4.89 ± 0.03 log CFU/cm^2 (mean ± SD) of non-planktonic

L. monocytogenes cells on SS after 3 h of contact with liquid broth agitated with a magnetic stir bar (de Oliveira et al., 2010). The liquid broth was used as the medium for bacterial attachment to the surface, which does not replicate initial contamination scenarios in dry environments. However, biofilm formation can occur in dry processing environments due to "microscopic surface wetness," where visibly dry surfaces are covered in microdroplets and liquid films (Orevi & Kashtan, 2021). A review of dry surface biofilms in the food processing industry contextualized the role of microscopic surface wetness and biofilm formation. While the processing environment is dry, wet biofilms can form and persist on equipment, especially on irregular surfaces, grooves, and hard-to-reach areas like nooks and crannies (Alonso et al., 2023). In the selected studies, microbial transfer was observed from a dry, biofilm contaminated surface to the target food powder. Similarly, modeling contamination from an inoculated powder to a dry food contact surface could be relevant for understanding sanitation practices in dry environments.

Multiple experiments have utilized the strategy of inoculating food contact surfaces with powder and have explored variations, including the use of spherical beads or inoculated powders as the vector of microbial transfer. A portion of a 2022 study by Liu, et al. investigated multiple transfers of *Salmonella* from #316 stainless steel and polypropylene beads (d=3.18 mm) to low-moisture foods and dry powders to evaluate the efficacy of system purges using uninoculated low-moisture foods. Approximately 11 log CFU/ml of *Salmonella* was adhered to the beads with an initial concentration of 8.09 ± 0.58 log CFU/cm^2 (mean ± SD) on #316 SS. 1 g of whole wheat flour, corn meal, and NaCl were separately mixed with three beads of each material type and had multiple exposures with uninoculated products. The change in *Salmonella* populations

on the surface of the #316 SS beads after a single whole wheat flour rinse was 0.34 ± 0.65 log CFU/cm^2 (Liu et al., 2022).

A recent experiment by Chen & Snyder used glass beads, spot inoculation, and milk powder as modes of pathogen transfer to food contact surfaces such as high density polyethylene (HDPE), #304 SS polished 2B finish, and rubber. 30 g of inoculated beads, separated by microorganism (*S. Enteritidis PT 30, E. faecium, L. innocua,* and *E. coli*) were combined with four sterile coupons of a target surface, sealed in a sample bag, and shaken for 5 min to inoculate the coupons, among other inoculation methodologies, and exposed to a custom-designed mechanical dry cleaning process. For powder inoculation, 10 g of dried inoculated milk powder was sealed in a sample bag with four coupons and mechanically mixed for 5 mins using a stomacher. Initial *Salmonella* populations on the glass-bead inoculated #304 SS coupons were 2.1 ± 0.8 log CFU/coupon (mean ± SD). After dry cleaning, the residual populations were 0.6 ± 0.6 log CFU/coupon, resulting in a 1.5 ± 1.2 log reduction (Chen & Snyder, 2023). In comparison, the milk powder method had initial populations of 3.3 ± 0.2 log CFU/coupon, post cleanings populations of 2.0 ± 0.4 log CFU/coupon, and a resultant log reduction of 1.2 ± 0.4 log CFU/coupon. The glass bead inoculation methodology had lower initial populations in comparison to the other inoculation strategies, highlighting the potential applications of powder-based inoculation methodologies onto SS surfaces.

Inoculating powdered food matrices to simulate cross-contamination onto food contact surfaces yields higher pathogen populations on surfaces compared to glass beads. However, this method might not transfer sufficient pathogens to the target surface to accurately represent potential cross-contamination scenarios. If the residual *Salmonella* populations on the target surface are too low, it becomes challenging to quantify sanitation parameters, as the inactivation

achieved by the technology may fall within the margins of experimental error. Thus, for the inoculated food powder strategy to be more widely applicable in dry sanitation, the initial populations within the powder should be approximately 7–8 log CFU/g to ensure high enough starting levels and to replicate the approximate initial populations used in other low-moisture food studies. This microbial load can be achieved in flour through a lawn-liquid inoculation methodology explored by Hildebrandt, et al. (2016), applicable only if wheat berries (flour precursors) are inoculated and equilibrated before milling, thus preventing any net moisture increase in the system.

In summary, the ideal method for inoculating dry food powder for use in dry sanitation studies should (1) minimize water usage, (2) use a relevant contaminated food product as the cross-contamination vector, (3) maintain high initial population levels to ensure adequate transfer to target food contact surfaces for sanitation experiments, and (4) keep water activity and relative humidity low throughout the experiment to mirror typical environmental conditions during processing.

Understanding how powdered food matrices adhere to food-contact surfaces could more accurately represent contamination scenarios in low-moisture food processing systems, offering insights for refining the dry powder inoculation method.

Powder Adhesion onto Food Contact Surfaces

In general, powder processing, involving mechanical actions such as sifting and grinding, produces dust that disperses and settles on all available surfaces, requiring cleaning (Figure 1).

Figure 1: Accumulated wheat meal on a milling attachment after milling inoculated and equilibrated wheat berries

Particle adhesion to surfaces primarily occurs through electrostatic attractions. Particles can become charged through friction from particle-to-particle collisions or from externally applied voltages, with electrical charge facilitating attraction between particles (Prasad et al., 2016). Charged particles can be generated in several ways, including the triboelectric effect, where electric charge transfer and generation occur through physical contact or friction (Bailey, 1998). Another method is corona discharge, involving the application of voltage to a powder to charge its particles (Bailey, 1998).

Charged particle adhesion to surfaces presents challenges in pharmaceutical processing and food production, especially within product lines (Ghori et al., 2015). In dry food processing systems, the accumulation of food particulate dust with triboelectric charge on food contact surfaces is widespread. However, the accumulation of charged powder on surfaces can also have advantageous applications in food processing; both electrostatic and non-electrostatic charging methods are often used for uniform coating of food products with spices and seasonings (Somboonvechakarn & Barringer, 2012). These coating principles can be deliberately applied to surfaces. Simply stated, by applying a voltage to a selected powder, the powder can adhere to an

electrically grounded surface due to the electric charge gradient between the particle and the surface. Powder coating, which involves uniformly applying and distributing powdered paint particles onto metal surfaces, is widely used in the automotive industry (Pilcher, 2001) and general manufacturing processes to enhance corrosion resistance (Fedrizzi et al., 2007).

Low-moisture food powder adhesion and removal from stainless steel surfaces has been recently studied. Klug, et. al, found that at lower relative humidities (20 and 40%), triboelectric charging significantly increased the adhesion rates of custom-fabricated all-purpose flour (U.S. Standard Mesh No.'s 60–80) on #304 electropolished SS coupons (2023) by using a simple triboelectric charging tube device. This was a novel approach to modeling equipment contamination in LMF processing systems. However, the study only used tribocharging as the method of charged particle adhesion to stainless steel surfaces and did not investigate the differences in composition and surface finish of the stainless steel.

Using electrostatic powder coating to adhere charged low-moisture food powders onto food contact surfaces could be a practical method for simulating the accumulation of food powder on equipment surfaces during processing. Incorporating *Salmonella* into food powders might offer an innovative way to affix inoculated food powders onto equipment surfaces. This approach could potentially secure high microorganism populations within dry foods to stainless steel food contact surfaces without introducing excess moisture, thereby altering pathogen behaviors such as desiccation and thermal resistance, and simultaneously simulating potential contamination scenarios. If the adhered powder exhibits high levels of *Salmonella* (>8 log CFU/g), it could leave sufficient populations on the target surface area to evaluate the effectiveness of new contamination methods. If there are consistent and replicable populations (>

4 log CFU/cm^2) remaining on the surface post-cleaning, it will be enough to determine significant differences in *Salmonella* populations before and after sanitation treatments.

When selecting the target SS surface, considerations should include the SS composition (grade), and surface finish. The roughness and microscopic grooves of the target surface could influence powder adhesion and microbial transfer.

Knowledge Gaps Within Current Literature: Dry Sanitation Methodologies

Considerations for evaluating new electromagnetic sanitation technologies should include exposure time, emitter-target distance, and radiation intensity for creating descriptive dosage models. In challenge studies, targeting a 5 log reduction in pathogen populations on foods and surfaces is recommended (National Advisory Committee on Microbiological Criteria for Foods, 2010). This study suggests that achieving a surface inoculation of > 5 log CFU/cm^2 and then reducing populations by 5 log would reduce surviving populations to below the limits of detection. Instead, aiming for a >3 log reduction might be more feasible with dry sanitation technologies, reflecting the reduced efficacy of sanitation in dry environments in comparison to thermal and chemical inactivation studies.

Variations in treatment duration, the distance between the radiation source and the target surface, and unspecified radiation intensity in prior studies (Table 1) limit the usefulness and applicability of these findings. In some prior research, exposure times extended to hours, impractical for continuous operation of processing lines. Differences in distance affect the ability to replicate experiments and compare them with other studies; as distance from the source increases, radiation intensity decreases due to the inverse square law. Additionally, not specifying

the radiation intensity or using incorrect units[1] for reporting it hinders comparisons across studies of UV-C technologies. Without the intensity value, it is impossible to calculate the radiation dose applied to microorganisms on the target surface. Clarifying the term "intensity" as it applies to UV-C and IR technologies could improve understanding of how radiation affects the target surface.

Consistently reporting sanitation parameters will propel sanitation innovations forward, offering a preliminary, evidence-based parameters for dosage modeling. This provides both industrial and academic researchers with a solid starting point for future experiments and the potential adoption of these technologies.

[1] The term *intensity* has different definitions and SI units depending on the scientific branch of inquiry. In physics, intensity is the power transferred per unit area (W/m^2). Confusingly, *intensity* has been used as a common term to refer to different quantities such *radiant intensity* (W/sr), *spectral intensity* (W/sr.m), *specific intensity (spectral radiance)* ($W/m^2/nm$), *radiance* ($W/sr.m^2$), *irradiance* (W/m^2), and *radiant exitance* (W/m^2), among others.

MATERIALS AND METHODS

Bacterial Strain and Culture Preparation

Salmonella enterica strains Agona (447967), Montevideo (488275), Tennessee (K4643), Enteritidis Phage Type 30 (ATCC BAA-1045), Mbandaka (698538), and Reading (Moff 1804180 were sourced from the Center for Food Safety and Applied Nutrition (Bedford Park, IL, US). Cultures were stored in a −80 °C cooler within an 80% (v/v) sterile glycerol solution prior to resuscitation.

To create stock and working plates, cultures were taken out of the freezer and left to thaw for 5 min. One loop (10 µl) of each strain was placed into individual 9 ml of room temperature tryptic soy broth (TSBYE) (BBL, BD, Sparks, MD, US) supplemented with 0.6% yeast extract (m/v) (Bacto, BD, Sparks, MD, US), then vortexed. The cultures were incubated at 37°C for 24 ± 2 h. After incubation, each strain was streaked onto individual plates (15 × 100 mm) of tryptic soy agar (Difco, BD, Sparks, MD, US) with 0.6% yeast extract (TSAYE) to isolate colonies to create a stock plate. Stock plates were incubated at 37°C for 24 ± 2 h, wrapped in Parafilm, and stored for up to six months.

From the stock plate, one colony of each strain was harvested aseptically using a 10 µl inoculum loop into individual 9 ml tubes of TSBYE, vortexed, and incubated at 37°C for 24 ± 2 h. One loop (10 µl) of culture was streaked onto individual TSAYE plates and incubated at 37°C for 24 ± 2 h to create a working plate. Working plates were wrapped in Parafilm and stored up to one month. To create additional working plates, individual colonies were harvested from the stock plate.

Wheat Berry Preparation and Inoculation

Hard red winter wheat and soft white wheat berries (Palouse Farms, Palouse, WA, USA) were purchased from an online retailer. An 80/20 ratio (m/m) of hard red winter wheat and soft white wheat berries were used as a basis for all-purpose wheat flour fabrication. The 80/20 wheat berry ratio was prepared in 1000 g batches for each experimental run. For the purposes of this research, an "experimental run" groups data and results gathered within the same day using the same batch of wheat berries. The wheat berry mixture was partitioned into a large 25.4 cm × 38 cm sample bag (Whirl-Pak LLC, Nasco Sampling, Pleasant Prairie, WI, USA), hand mixed, and spread into an even layer on a quarter-sheet aluminum pan within a custom equilibration chamber, set to 45% relative humidity, for 48 ± 2 h to equilibrate to a water activity (a_w) ~0.45 prior to inoculation.

1 ml of each *Salmonella* culture was pipetted onto large (150 mm × 15 mm) TSAYE plates and spread using an L-shaped spreader. The lawn plates were incubated at 37°C for 24 ± 2 h. After, the lawns were harvested in 9 ml of 0.1% (m/v) buffered peptone water (BPW) (Difco, BD, Sparks, MD, US) using an L-shaped spreader. The harvested cultures were dispensed into a single 250 ml centrifuge bottle using a 5 ml glass auto-pipette. The combined *Salmonella* cultures were centrifuged for 15 min (SLA-1500, 4500 rpm, 3000×*g*). After centrifugation, the supernatant was poured off the inoculum, and the pellet was resuspended in 25 ml of BPW. The initial *Salmonella* populations in the inoculum were ~11.4 log CFU/g.

The inoculum was pipetted to the uninoculated, equilibrated wheat berry mixture. The sample bag containing the wheat berries was sealed and hand massaged for 5 min to distribute the inoculum on the surface of the berries. After, the berries were allowed to dry on a sterilized half sheet plastic tray lined with absorbent pads for 15 min. This step removed excess moisture

from the inoculum and facilitated equilibration of the berries. Once dried, the berries were placed back into the original sample bag, then transported to a custom equilibration chamber. Here, they were evenly distributed on an aluminum half-sheet pan (457 × 330 × 25 cm). They underwent further equilibration at 45% relative humidity for an additional 48 ± 2 h, achieving a water activity level of approximately 0.45.

The a_w of the uninoculated and conditioned wheat berries was measured prior to inoculation using a water activity meter (Model 4TE, Decagon Devices, Pullman, WA, USA). Samples of background microbial populations for each wheat berry variety were plated onto tryptic soy agar (TSA) (Difco, BD, Franklin Lakes, NJ, US).

Wheat Milling and Sieving

The inoculated wheat berries were milled and sieved to simulate a worst-case initial contamination scenario where contaminated wheat berries were used for flour fabrication.

Figure 2: A stand mixer with a grinding attachment

A KitchenAid mixer (model K5-A, KitchenAid, Troy, MI, US) and milling attachment were placed within in a laminar flow biosafety cabinet (Figure 2). 1000 grams of the inoculated

wheat berry mixture was poured into the grinding attachment. The berries were ground into the KitchenAid mixing bowl at mixer speed 4 (~125 rpm). The mixing bowl was suspended using a plastic sample bag holder to accrue the ground wheat meal and prevent unnecessary spread of contaminated products. After grinding, the bowl containing the wheat meal was transferred into a 1.82 m × 1.21 m chemical fume hood (NLS 637, Fisher American, Rockford, IL, US) that housed a mechanical sieve (Model H-4330, Humboldt Manufacturing Corporation, Elgin, IL, USA). The relative humidity of the hood (~33% for all experimental runs) was displayed using a digital hygrometer (model TP50, ThermoPro, Inc., Duluth, GA, US).

The wheat meal was sieved for 5 min using US standard mesh sizes No.'s 20, 70, 100 (Figure 3) and 200 to fabricate all-purpose flour from the wheat meal, following 21 C.F.R 137 requirements (Title 21 C.F.R. § 137.105) First, wheat meal (~300 g) was added to the No. 20 sieve along with a small rubber ball to promote proper sieving. The meal was sieved in portions since 1000 g could not be sieved simultaneously. On average, the wheat meal took three 5 min cycles to sieve all 1000 g of the fabricated wheat meal.

Figure 3: Sieving system used for flour fabrication. From top to bottom, a lid, a U.S. Standard No.'s 20, 70, 100, and 200 mesh, followed by a sieve bottom

To follow US standards for flour, all particles that did not pass through the No. 70 mesh (> 212 µm) were discarded into a biohazard container. After each 5 min sieving cycle, particles that passed from the No. 70 mesh to the No. 200 mesh were classified as "flour" and collected into an 18 oz. sample bag for later use using a sterile spoon. From the initial 1000 g of wheat meal, approximately 80–100 g of all-purpose flour was produced through the milling process, intended for utilization in the powder coating inoculation methodology section. Coarse particles that could not be classified as flour were disposed of after the sieving process.

To assess the effects of sieving on *Salmonella* populations adhering to the wheat berries throughout the milling process, triplicate samples of the berries were collected before grinding, after grinding, and from each sieve following a single 5 min sieving cycle.

Stainless Steel Coupon Preparation

Twenty stainless steel circular rounds (14 gauge, 0.19 cm thickness, 6.43 cm diameter) were custom fabricated (Stainless Supply, Monroe, NC, USA) with three grades and surface finishes (#304 brushed, #316L brushed and #304 mirror finish). The circular coupons were used to simulate metal equipment surfaces in a production line. One coupon from each stainless steel grade and finish was set aside from the sampling stock for reference and imaging purposes (Figure 4).

Figure 4: #304 brushed finish (left), #316L brushed finish (center), and #304 mirror finish (right) stainless steel coupons

The mass of each coupon was measured using a benchtop balance (OHAUS Explorer, model E02140, Parsippany, NJ, US), with the measurement recorded and hand-etched near the rim of each coupon using a handheld rotary tool (Dremel, model 395, type 5, Robert Bosch Tool Corporation, Mount Prospect, IL, USA).

Before each experimental run, the coupons were sterilized by autoclaving at 121.8°C for 30 min (121348 Pa) to inactivate *Salmonella* residues from previous experiments. Inside a chemical fume hood, the coupons were placed into a 1 quart metal paint can, an acetone-safe container holding 250 ml of acetone. The can was sealed using a rubber mallet, and the coupons were submerged for 15 min to eliminate surface resides, following procedures established in prior work (Suehr, 2020) (Figure 5).

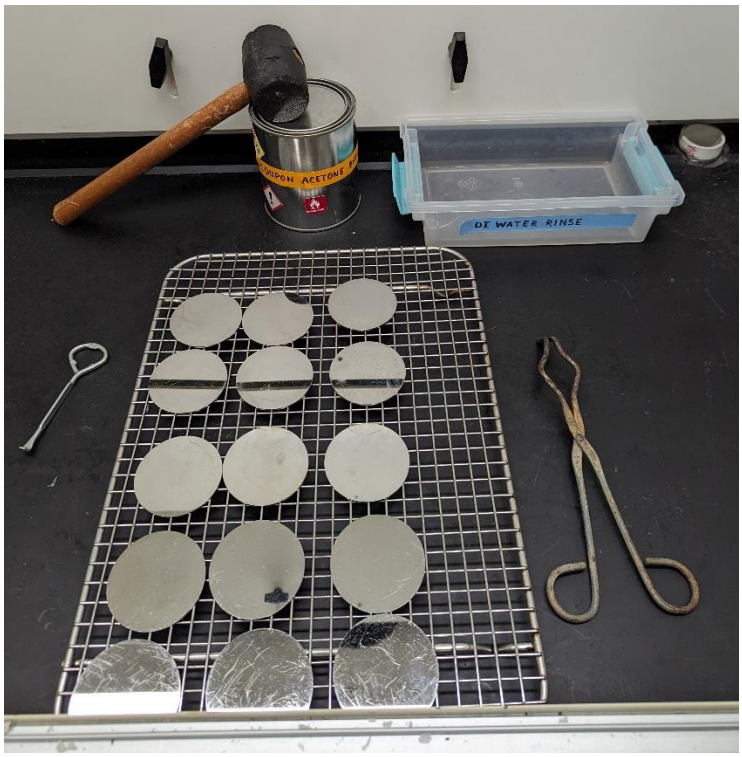

Figure 5: Stainless steel coupon preparation

The coupons were first removed and placed onto a wire cooling rack for 1 min to facilitate acetone evaporation. Subsequently, they were submersed in a container filled with deionized water for one minute, ensuring the removal of any residual acetone from their surface. After, the coupons were placed evenly distributed on the wire rack. Excess water was removed using kimwipes and paper towel and transferred to a drying oven (~100°C) for 10–30 min to dry completely and prevent rusting. Once dried, the coupons were allowed to cool to room temperature before use in electrostatic powder coating.

Evaluation of Electrostatic Powder Coating Inoculation Methodology

The fabricated all-purpose flour was applied to stainless steel surfaces using a powder coating gun. The goal was a target population of > 5 log CFU/cm^2 on the coated coupons and > 4 log CFU/cm^2 on the surface of visibly cleaned coupons.

The powder coating set-up was housed within a modified silica blasting chamber (Model SBC 420, Atlas Auto Equipment, Greenfield, IN, USA), which contained a clamp stand, a 46.9 cm x 37.8 cm x 28.3 cm gasket box with the front panel removed (model 1933, Sterilite Corporation, Townsend, MA, US), a small handheld vacuum (model 47R51, Bissell, Walker, MI, US), a humidity controller (model IHC-200, INKBIRD Tech. C.L., Shenzhen, CN), and a humidifier (model VUL520W, Kaz USA, Incorporated, Malaborough, MA, USA) (Figure 6).

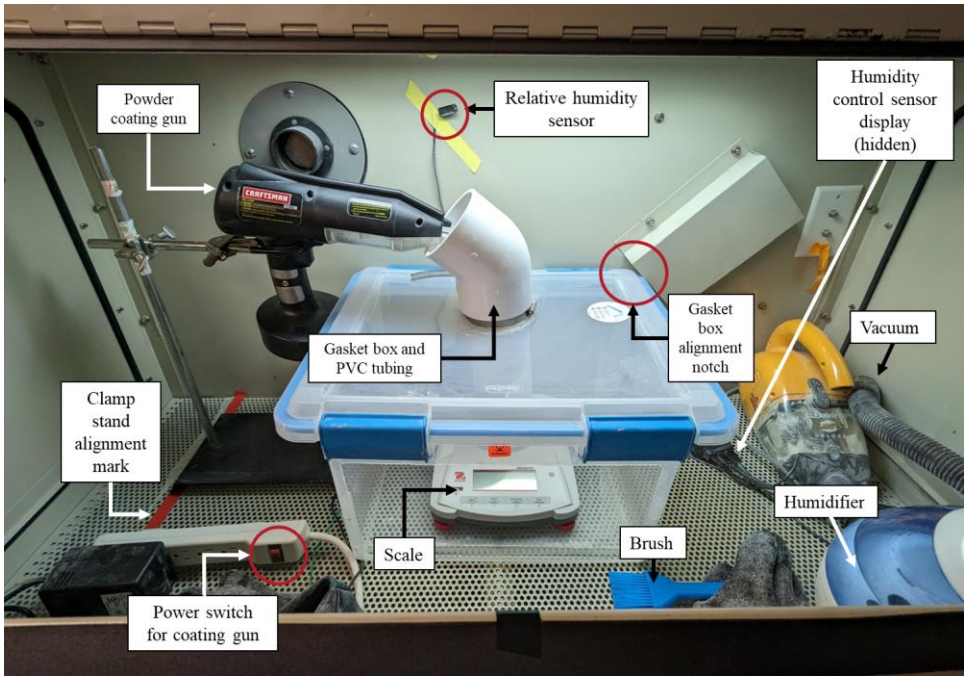

Figure 6: Labeled photo of equipment used for electrostatic powder coating within an equilibrated chamber

During experimental runs, the gasket box was secured in position using the metal notch on the chamber's far back wall while the clamp stand's position was maintained with a reference line marked by tape. The combined 45° angled PVC pipe and 20.3 cm straight PVC pipe (7.62 cm nominal diameter) localized the area of powder accrual onto the surface of the portable benchtop scale and the SS coupon (OHAUS Navigator, model NV223, Parsippany, NJ, USA).

To inoculate the stainless steel coupons, the powder coating gun (model 917288, Craftsman, Towson, MD, US) was suspended 39 cm from the bottom of the chamber using a clamp stand. The grounding wire from the powder coating gun power source was fixed to metallic surfaces on the scale using a piece of electrical tape. The relative humidity inside the powder coating chamber was maintained at 45% using a humidity controller and a humidifier to represent average low-moisture food processing conditions. The initial relative humidity within the chamber was recorded at the beginning of each experimental run.

40 g of the inoculated all-purpose flour was added to the coating gun's powder reservoir. For mass measurements during powder coating, a portable benchtop laboratory scale was used. The scale was tared, and a coupon was placed and tared on it. The powder coating gun's trigger was secured in position with electrical tape and activated by an on-off switch on a separate power strip.

Upon activation, the inoculated wheat flour in the powder cup was expelled through the high voltage tip of the gun. It then dispersed through the PVC pipe apparatus, primarily depositing onto the selected coupon type and to a lesser extent on the sensing surface of the scale. Once the scale registered a mass of 0.2–0.3 g (accounting for both flour and air pressure), the powder coating gun was turned off. Any excess flour on the surface of the scale was brushed off using a soft-bristled, 5 cm wide pastry brush with polyester bristles (Model 5552503, Vikan, Skive, DK), leaving only the flour adhered to the coupon, with a target value of approximately 0.1 g, was documented in a laboratory notebook.

#304 and #316L SS brushed finish coupons were coated with inoculated flour (n=48). Half of the coated samples were transferred into sample bags without a brushing step as negative controls. Subsequently, the remaining half were brushed to a "visibly clean" state using the soft-

bristled brush described earlier, with the brush being alternately chosen from a stock of two per each experimental run. In this experiment, “visually cleaned” was defined as the absence of particles visually detectable to the naked eye, a criteria used in prior research (Daeschel et al., 2023; Moretro et al., 2020). All experimental runs were conducted in triplicate.

To create a visibly cleaned surface, the coupon was smoothly brushed ten times from top to bottom, starting from the northern edge of the coupon to the southern edge, followed by a 180° rotation of the brush to use the opposite side for brushing ten times from left to right from the western coupon edge to the eastern edge (Figure 7). The visibly cleaned coupon was placed aside into a small metal tray and removed from the chamber. The assumed mass of remaining particles was 0.01 g, 1/10 of the adhered mass for *Salmonella* population calculations since trace amounts of flour particles remained on the surface after visibly cleaning.

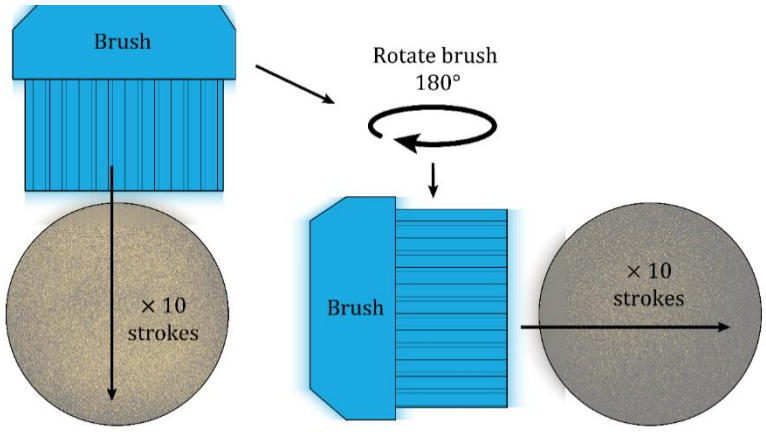

Figure 7: Brushing protocol to create visibly cleaned coupons

Microscope images of the untreated, coated, and visibly cleaned coupons were taken using a trinocular microscope (series SM-1T, AmScope, Irvine, CA, US) with an attachable camera (model MU1000-HS, AmScope, Irvine, CA, US), at 10× magnification.

Application of UV-C, Far UV-C, and IR Radiation

For the sanitation experimentation, the powder coating inoculation methodology was applied to #304 SS brushed and mirror finish coupons (Figure 8) to evaluate the effect of surface finish on sanitation efficacy. Samples (n=206) were visibly cleaned using the same methods described in Figure 7. Each experimental sanitation run was conducted in triplicate. Negative controls (n=68), which were coated and visibly cleaned, were used for comparison with treated samples.

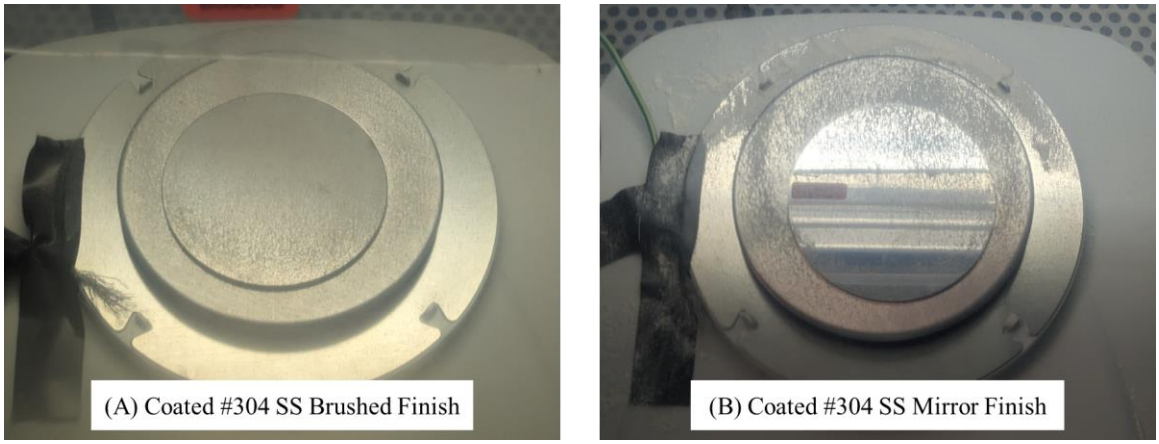

Figure 8: Coated #304 SS brushed finish (A) and #304 SS mirror finish (B) coupons

After being taken out of the powder coating chamber, the coupons were brushed once from top to bottom (northern edge to southern edge) to clear off any additional particles that clung to the coupon surface from their time inside the chamber after being visibly cleaned. The underside of the coupon was then carefully wiped a delicate task wipe that had been sprayed with 75%, 200 proof ethanol, to inactivate any residual *Salmonella* populations that could affect the results following the sanitation treatment. Subsequently, the prepped coupon was placed into a labeled plastic sample weigh boat, facilitating safer and more efficient transport from the powder coating chamber to the chamber where UV-C, Far UV-C, and IR radiation technologies were applied for sanitation.

An equilibration chamber (Economical glove box, model 34788-00, Cole-Parmer, Vernon Hills, IL, USA) was used to house the sanitation technologies used in the experiment (Figure 9). The equilibration chamber was set to approximately 45% relative humidity and verified before treatment using a precision handheld psychrometer (model RH 390, Extech Instruments, Knoxville, TN, US).

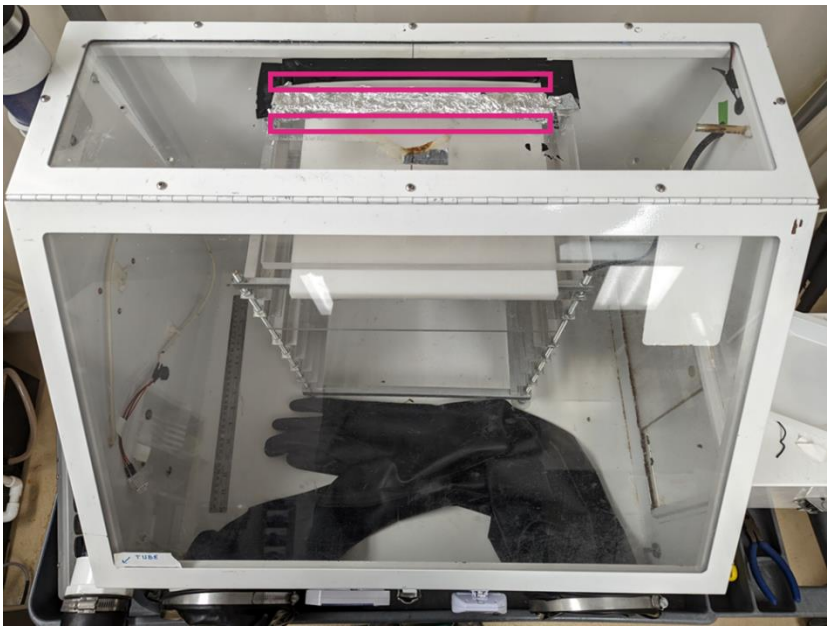

Figure 9: The sanitation treatment chamber with racks and two slots (8 cm × 2.2 cm) (in pink) on top of the chamber for housing the selected technologies

Two 8 cm × 2.2 cm slots were cut into the top plexiglass sheet to accommodate the sanitation technologies, facilitating easy removal and replacement of each sanitation device as required by different experimental run. For each experiment, the chamber included a repurposed metal sample holding rack with metal notches, an HDPE cutting board (25.4 × 25.4 × 1.27 cm), and three plexiglass sheets (31.1 × 22.8 × 0.5 cm). The distance from the sanitation device was adjusted using these sheets, accommodating the slight variations of the suspended height of each emitter. Distances of 10 cm and 15 cm from the device were measured and fixed by adjusting the metal notches on the wire rack, considering the height of the sheet under the sample (Figure 10).

The sample at a 5 cm distance was positioned on one HDPE sheet atop three plexiglass sheets, while those at 10 and 15 cm distances were set on one plexiglass sheet within their designated metal notches.

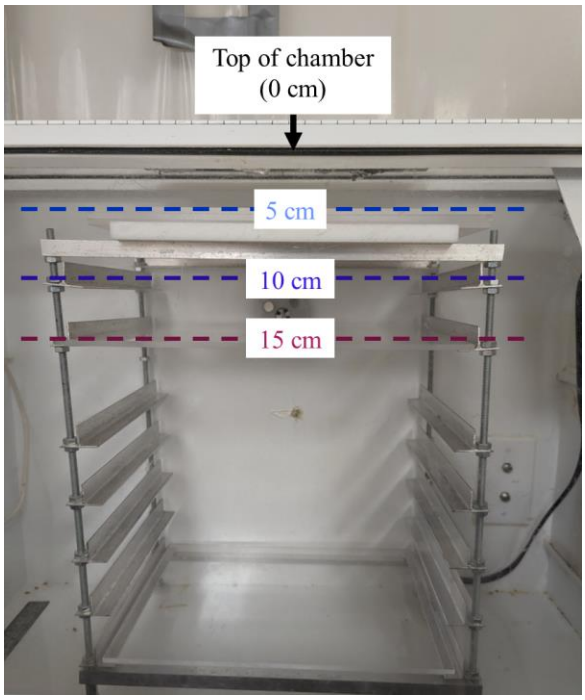

Figure 10: Distance measurements within the sanitation chamber

To generate UV-C at a wavelength of 254 nm, a Biolux® 6 W UV-C irradiating strip fixture (model 40-1106, Atlantic Ultraviolet Corporation, Hauppauge, NY, US) and a mercury bulb were used. For far UV-C at a wavelength of 222 nm, a 40 W Excimer Far UV-C lamp (model FRL-EMY-8-40W-FUVC-KT-120V, Larson Electronics, Kemp, TX, US) using corona discharge was used. IR was generated by a 500 W quartz infrared heater lamp (model QIH-120-500T/S, Ushio America Incorporated, Cypress, CA, US) that emitted IR from a horizontal burn position. The IR bulb was housed within a custom fabricated SS fixture. The fixture was fabricated from a 31.8 × 5.1 × 0.2 cm #303 SS bar, with a 22.2 cm rectangular hole removed from the bottom for IR bulb installation by the Department of Biosystems and Agricultural Engineering Fabrication Shop (Michigan State University, Esat Lansing, MI, US). Eight 2.54 cm

diameter holes were cut into the stainless steel bar to allow for heat removal. The exposed wires from the IR bulb were mounted between heat-resistant ceramic standoffs (1.9 cm × 0.95 cm diameter) and secured using 1.9 cm long Philips head screws and 0.95 cm diameter #316 stainless steel washers. High-temperature stranded wires with fiberglass and mica insulation were used to connect the IR bulb to a variable voltage controller switch (model 55150-SU E1030I, Sunlite, Brooklyn, NY, US) and then to a three-pronged power cord (Figure 11). The voltage was set to a maximum of 120 V for all experimental runs that required IR. To prevent overheating, excess heat from the IR device was dissipated using a 6.6 W fan (97 mm × 33 mm BBQ Blower Fan, WDERAIR, Shenzhen Shaoyuanqiao Technology CO. Ltd., Shenzhen, CN), which directed air flow from right to left through the metal housing and over the bulb. Beneath the IR fixture, there was a 15.2 cm × 15.2 cm Ultra-High-Temperature Quartz Glass sheet capable of withstanding temperatures up to approximately 1150 °C. This sheet mitigated the impact of heat on the plexiglass sheet on the top of the equilibrated chamber (Figure 9), and the impact of cooling air flow onto the sample coupon.

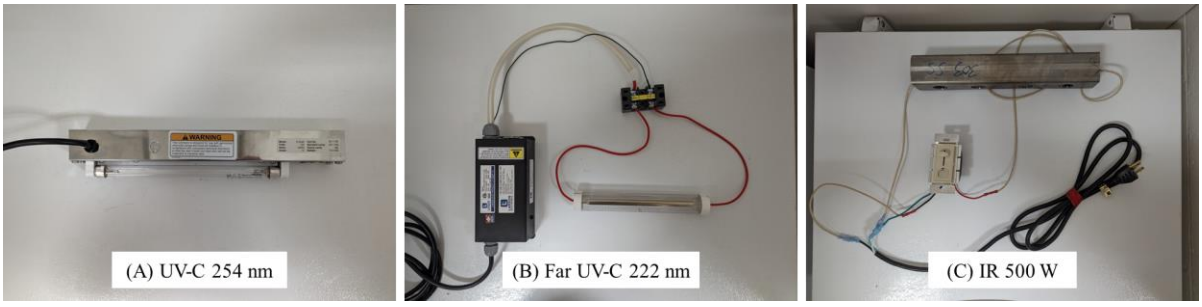

Figure 11: UV-C 254 nm device (A), Far UV-C 222 nm excimer lamp (B), and infrared lamp and ballast (C)

Visibly cleaned coupons were placed in a sample boat within the chamber and positioned on the wire rack at the chosen distance from the emitter.

Each device was controlled using a power strip. When the device was powered on (Figure 12) a handheld timer was started concurrently to mark the length of exposure. The device was

turned off once the predetermined exposure time was reached, as indicated by the timer (Table 2).

Table 2: Treatment factors applied to stainless steel coupons

Technology	Distance From Emitter	Length of Exposure (min)
UV-C 254 nm	5	[0.33, 0.66, 1, 2, 3, 5, 10, 20]
	10	[0.33, 0.66, 1, 5, 10]
	15	[0.33, 0.66, 1, 2, 3, 5, 10]
Far UV-C 222 nm	5	[0.33, 0,66, 1, 2, 3, 5, 10, 20]
	10	[0.33, 0.66, 1, 5, 10]
	15	[0.33, 0.66, 1, 2, 3, 5, 10]
Infrared Radiation	5	[1, 2, 3, 5, 10, 20, 60]
	10	[1, 5, 10, 60]
	15	[1, 2, 3, 5, 10, 60]

The experimental design of the sanitation portion explored the sanitation method, with three levels (UV-C, Far UV-C, IR), the distance from the emitter (i.e. intensity) with three levels (5, 10, 15 cm from the emitter), and the length of exposure, which ranged from 10 s to 60 mins (Table 2). Due to the exploratory nature of the sanitation experimentation, various exposure times were tested and selected to meet the > 3 log CFU/cm^2 reduction goal on the stainless steel coupons.

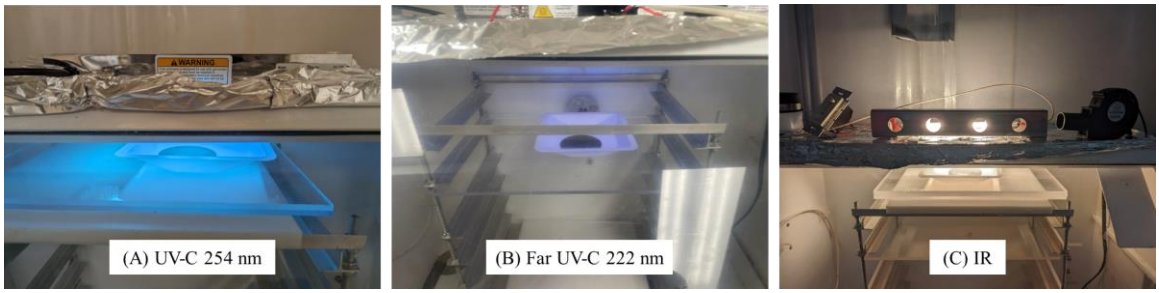

Figure 12: Sanitation of visibly cleaned SS coupons using UV-C (A), Far UV-C (B), and IR devices (C)

After the target exposure time was reached, the weigh boat and treated coupon were removed from the chamber, cooled as necessary, and transferred into labeled 18 oz sample bags.

Changes in relative humidity changes following a 60 min IR treatment were monitored using a handheld psychrometer, with readings taken at 10 min intervals.

Intensity Measurements

Intensity refers to the power (radiant flux) per unit area of electromagnetic radiation reaching a surface, measured in W/m^2. It has the same units as *irradiance*, the radiant flux received by a surface per unit area, and *radiosity,* the radiant flux exiting a surface per unit area. In this study, intensity refers to the irradiance of SS coupons exposed to UV-C, Far UV-C, and IR radiation, since the radiation impinges on the surface (and microorganisms) from a single direction.

The theoretical intensity of the energy emitted from the radiation source to a target surface can be described using the inverse-square law (Equation 1) with the assumption that energy is emitted in a spherical manner from a point source to a surface. The intensity of the radiation on a surface at a specified distance from the emitter was calculated from the following equation (1):

$$I = \frac{P}{A} = \frac{P}{4\pi r^2} \quad (1)$$

Where I is the intensity (W/m^2), P is the power of the emitter (W), A is the surface area of the sphere (m^2), and r is the distance from the emitter to the target surface (m). It is common in literature to report UV-C intensity values in mW/cm^2.

The UV-C radiation intensity for both UV-C devices was measured using a UV-C light meter (Model UV512C, General Tools & Instruments LLC, Secaucus, NJ, US). Intensity values were filtered as average values on the device display prior to recording the intensity measurements using the AVG function within the device.

A #304 brushed finish SS coupon was traced onto a plastic sample boat to model UV-C exposure on the surface of the coupon (Figure 13). 1 cm circles were cut on the model coupon tray at the center of the coupon, 1.6 cm from the center, and 3.2 cm from the center, corresponding with the middle of the coupon surface, the mid-edge, and outer edge, respectively, to allow access for the 1 cm diameter sensing region of the UV-C light meter.

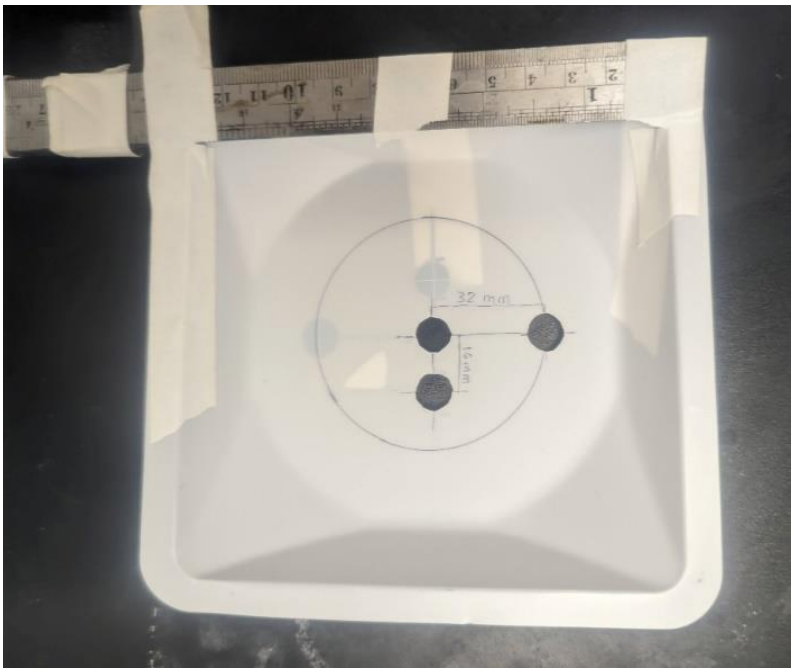

Figure 13: Simulated coupon surface used for UV-C and Far UV-C intensity measurements

The sample coupon surface was placed at (5, 10, 15 cm) from the emitter using a clamp stand within the equilibrated sanitation treatment chamber (Figure 14). The intensity of incident energy at 5 cm was recorded for all technologies with several variations. Initially, the intensity was recorded with a "cold-start," meaning the intensity measurement started concurrently with powering of the technology. Then, additional measurements were taken after the device was powered for 5 min to determine the intensity after a 5 min "warm-up" time.

For UV-C, the intensity at separate locations on the coupon were measured using the "cold-start" method to determine intensity variations across the surface, using a method adapted from Bolton & Linden (2003).

The intensity values reported in this study for dosage modeling were recorded under "cold-start" conditions to represent the probable use of the technologies on the processing line, where "warm-up" time may be minimized or disregarded to reduce the downtime of equipment for sanitation.

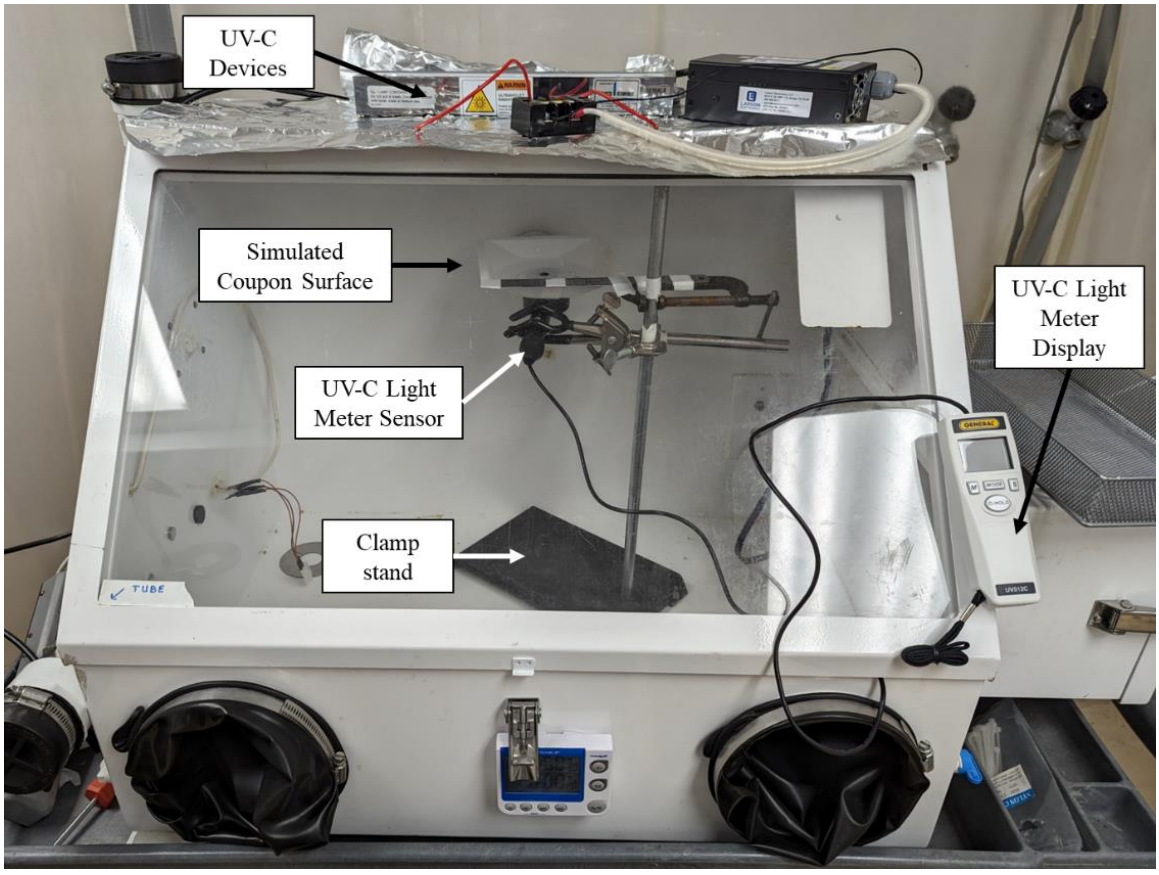

Figure 14: UV-C intensity measurement set-up within the sanitation treatment chamber

The experimental IR intensity (W/cm^2) was calculated using an alternative method based on heat transfer principles, considering the primary effect of IR on a surface is heating. Given its

minimal thickness, the coupon was considered as a lumped system. The equation (2) below characterizes the total energy absorbed by the coupon exclusively through its surface:

$$q = mc_p(T_{final} - T_{initial}) \quad (2)$$

Where q is the energy emitted to the coupon surface (J), m is the mass of the coupon (kg), c_p is the specific heat of the #304 SS. T_{final} is the recorded temperature (°C) of the coupon at the point where the percent change in temperature per minute was less than 10%. $T_{initial}$ is the starting temperature of the coupon (°C). To calculate the IR intensity on the surface, q was divided by both the surface area of the coupon and the time to reach T_{final}.

The intensity of the emitted infrared radiation was recorded using a modified temperature measurement device (Figure 15). A 1.1 mm hole was partially drilled into the center of a #304 brushed finish coupon to implant the tip of a 36 G T-type thermocouple which was used to record the incident temperature at the surface of the coupon. The thermocouple tip was secured in the hole using autoclave tape, and the hole was then filled with heat-resistant thermal paste to remove air that could skew temperature measurements (Figure 15 A). The coupon was encased within high-temperature resistant fiberglass insulation (Figure 15 B) to shield the thermocouple wire from high temperatures. A rectangular channel was cut into the insulation to route the thermocouple wire out of the equilibrium chamber. Intensity measurements were recorded over 60 min with a sampling rate of 2 s using a temperature data logger (model RDXL4SD, OMEGA Engineering Incorporated, Norwalk, CT US).

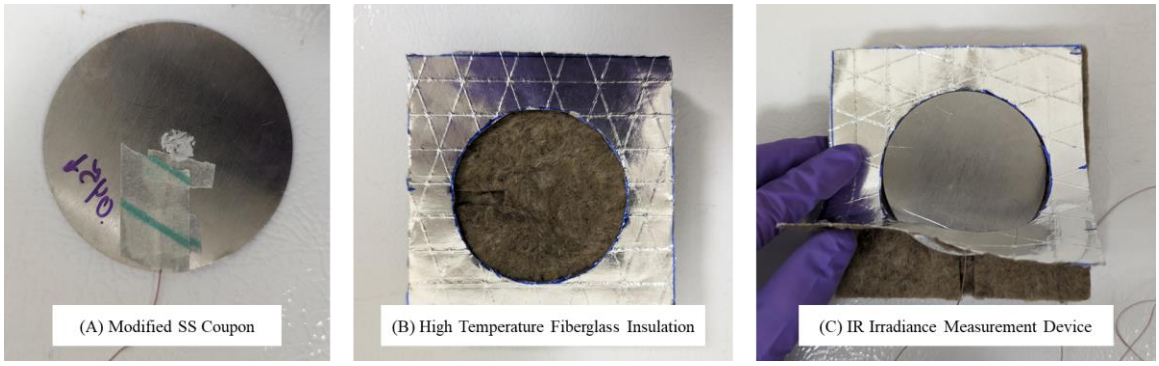

Figure 15: (A) Modified #304 SS coupon with 0.11 diameter cm hole with affixed thermocouple, (B) A 10 x 10 x 2.5 cm block of high temperature fiberglass insulation with a circular indentation cut out to house the coupon in the center, and (C) IR irradiance measurement device with a visible channel

Dosage Calculations

Dosage refers to the intensity (W/m^2) of incident electromagnetic radiation impinged on a surface over a measured length of exposure (s). A more accurate term for dosage, especially for UV-C radiation, is *fluence* or *radiant exposure,* since incident UV-C light passes through most microorganisms with a minimized percentage of absorption (Bolton & Linden, 2003). In general, dosage refers to the total incident energy *absorbed* by a surface. In this study, dosage refers to the fluence of SS surfaces exposed to UV-C, Far UV-C, and IR radiation. Dosage can be simply described Using Equation 3 (Demeersseman et al., 2023):

$$Dosage = Intensity \times length\ of\ exposure \quad (3)$$

Where dosage is J/m^2, intensity is W/m^2, and length of exposure is in seconds. For the purposes of this experiment, dosage was reported in mJ/cm^2 to remain consistent with generally used units of intensity (mW/cm^2).

Plating and Enumeration

5 ml of BPW was added aseptically to all bagged stainless steel coupon samples, whether the samples were coated, visibly treated, or exposed to dry sanitation technologies. The bags were closed and hand massaged for 1 min to distribute the diluent across the surface of the

coupon and to collect any remaining flour particles. Additional samples of *Salmonella* populations on the soft-bristled brush were diluted in 5 ml BPW. The samples were serially diluted in 9 ml buffered peptone water, plated onto modified tryptic soy agar (MTSA) (+ 0.05% ammonium ferric citrate (Alfa Aesar, Tewksbury, MA, US) + 0.03% sodium thiosulfate pentahydrate (Fisher Chemical, Waltham, MA, US), (Difco, BD, Franklin Lakes, NJ, US) and incubated at 37 °C for 48 ± 2 h. Any black colonies found on the surface of the media were considered as a colony forming unit and were recorded within a laboratory notebook. Population counts and log reductions were recorded and calculated using a spreadsheet, Microsoft Excel (version 2404 Microsoft, Redmond, WA, US). To determine the limits of detection (LOD), one colony forming unit at the highest dilution level used within the study was used to calculate the corresponding populations (log CFU/cm^2). For samples with a single serial dilution that plated the entirety of the diluent, the limit of detection for *Salmonella* was −1.5 log CFU/cm^2. For samples with multiple serial dilutions, the limit of detection was −1.1 log CFU/cm^2. The LOD for samples with multiple serial dilutions was lower because not all the diluent was plated onto agar plates. The residual diluent in the sample bag contained *Salmonella* populations that were not enumerated. In contrast, the single dilution samples plated all of the diluent on agar plates, enumerating all *Salmonella* that were present within the diluent and sample bag.

Statistical Analysis

General descriptive statistics for *Salmonella* populations (mean, standard deviation, standard error) were generated using the descriptive statistics procedure. *Salmonella* populations were analyzed using a general linear model procedure (GLM) within ANOVA to determine the significance (α=0.05) of factors and their interactions. ANOVA was conducted on the milling process (grind, sieve size), coating experiments (SS grade, SS finish, brushing treatment), and

negative control samples (experimental run) to determine significance of factors. Following this, all-pairwise comparisons of the means were conducted using Tukey's T-test (α=0.05) to reduce the chance of type I error through the comparison of multiple variables.

The relationship between dosage and *Salmonella* reduction for each technology (UV-C, Far UV-C, and IR) was described using a linear regression model. The quality of the model was assessed using reported R^2 and RMSE values. Model parameters and their 95% confidence intervals were calculated from the linear regression. The estimated slope parameter and its 95% confidence interval was used to calculate the dosage required for a target sanitation efficacy (log reduction, CFU/cm^2). Analysis of covariance (ANCOVA) was employed to determine whether the sanitation technology used had a significant effect on the predicted dosage model (α=0.05). The data analysis was conducted using Minitab, a commercial statistical analysis software (Minitab 21, State College, PA, US).

RESULTS

Grinding and Sieving

Following the inoculation of the raw wheat berries, the impact of the milling process on *Salmonella* populations were observed. There was a significant reduction (p=0.007) after the wheat berries were ground into wheat meal (Figure 16).

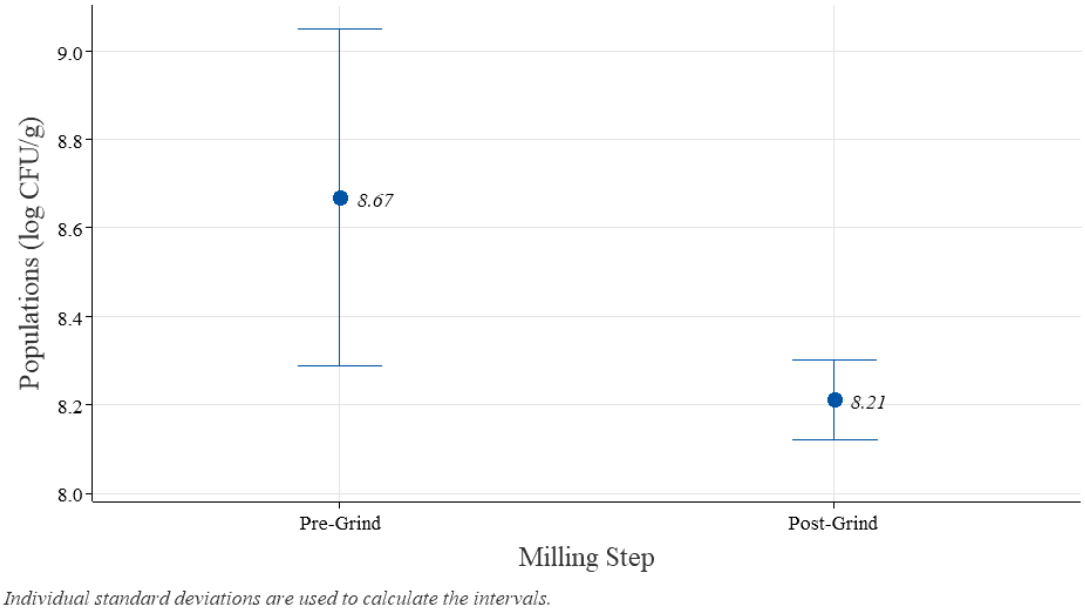

Figure 16: 95% confidence intervals of wheat berry Salmonella populations throughout the milling process. Pre-grind (unground berries) and post-grind (berries milled into wheat meal). Mean populations are listed to the right of each interval plot

After the sieving process, more samples of inoculated flour were collected from individual sieves. The factor of mesh size was found to be significant (p=0.034), with pairwise comparisons showing that samples from No. 200 mesh had significantly lower *Salmonella* populations than those from No. 20 mesh (Figure 17).

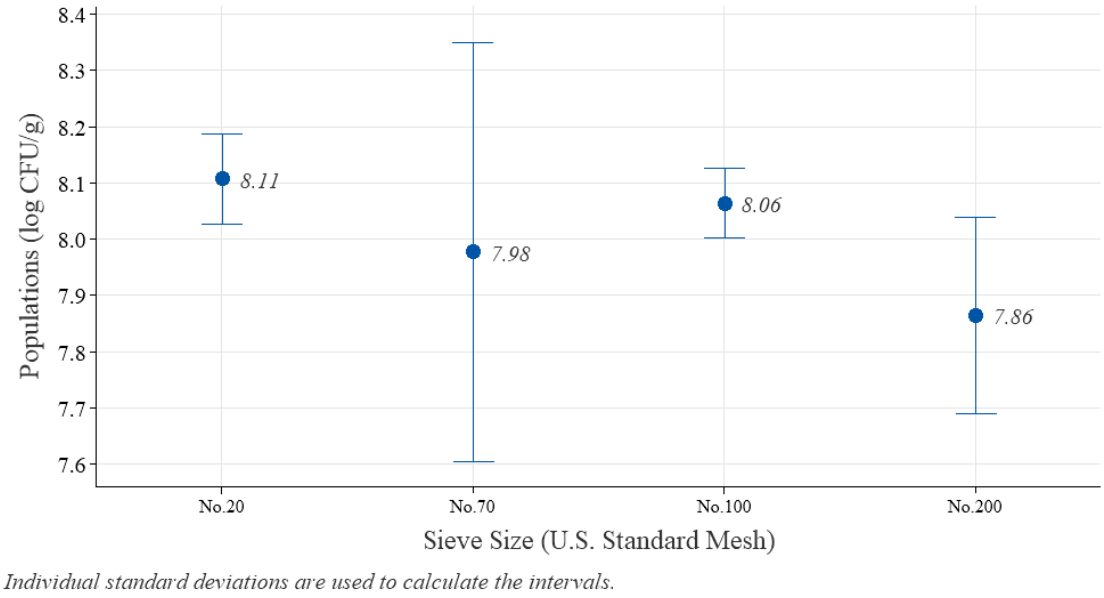

Figure 17: 95% confidence intervals for wheat meal and flour particles within each respective U.S. Standard Mesh after one 5 minute sieving cycle. Mean populations are listed to the right of each interval plot

After completing the grinding and sieving process, the average *Salmonella* populations in the fabricated flour prepared for the powder coating experiment were 7.94 ± 0.11 log CFU/g, indicating a loss of <1 log CFU/g during milling.

Evaluation Of Powder Coating Inoculation Methodology

The electrostatic powder coating device was able to adhere inoculated flour on stainless steel surfaces (Figure 18).

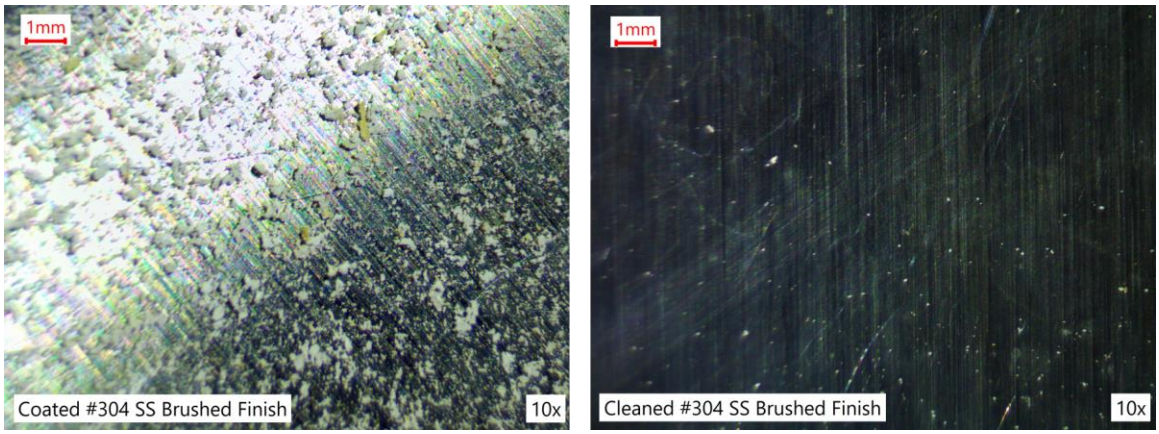

Figure 18: Microscopic images of coated (left) and brushed to visibly clean (right) #304 SS, brushed finish, at 10X magnification

Before starting sanitation trials, the effectiveness of the dry inoculation methodology was assessed. Preliminary trials were conducted to evaluate the impact of stainless steel grade, finish, and brushing to visually clean state on *Salmonella* populations. ANOVA showed there were no significant differences in coated and brushed populations between each stainless steel grade (p=0.22). The *Salmonella* populations on the coupons were significantly different ($p<0.001$) after visibly cleaning, with ~ 4 log CFU/cm^2 remaining on the surface (Figure 19). There were no significant differences in *Salmonella* populations adhered to #304 SS brushed finish and mirror finish coupons (p=0.480).

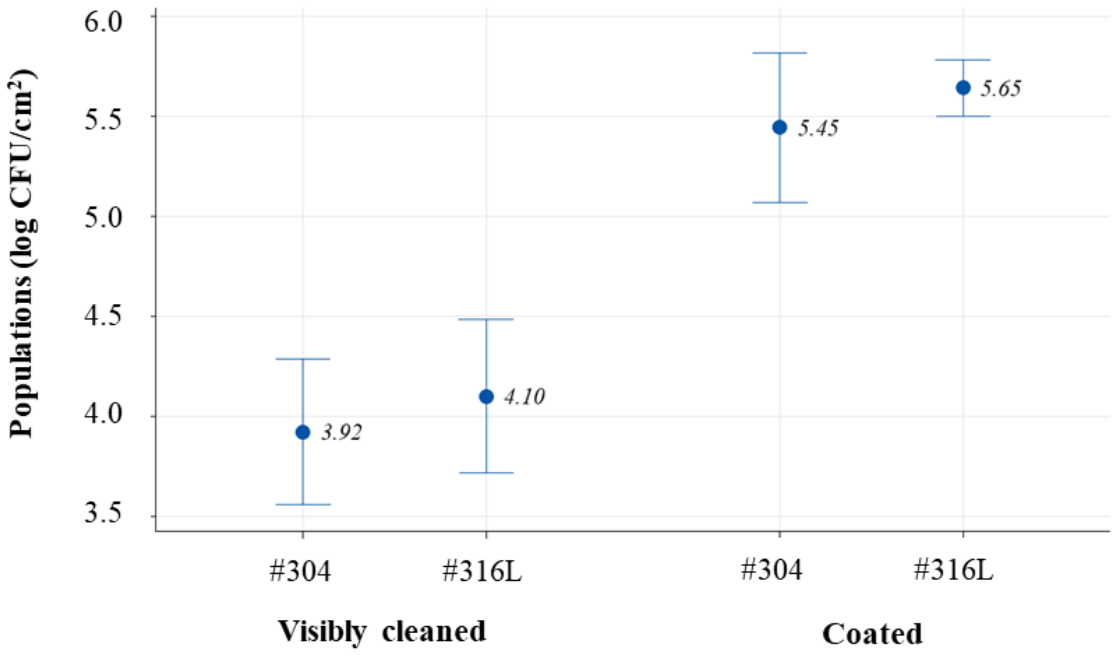

Figure 19: 95% confidence intervals of Salmonella populations on coated and visibly cleaned stainless steel coupons

The consistency of *Salmonella* application on SS coupons for sanitation experimental runs was measured using a one-way ANOVA on inoculated, non-irradiated control samples (Table 3). There were no significant differences in negative control populations between runs within the sanitation portion of the experiment (p=0.06). The mean *Salmonella* population for all visibly cleaned non-irradiated control samples were 3.09 ± 0.16 log CFU/cm^2 (mean ± SD).

Table 3: Descriptive statistics and 95% confidence intervals for inoculated, non-irradiated control samples for different sanitation experimental runs

Factor	N	Mean	SD	95% CI
Run 1	3	3.0279	0.0967	(2.8679, 3.1878)
Run 2	3	2.9468	0.1723	(2.7869, 3.1068)
Run 3	3	3.2987	0.1542	(3.1388, 3.4586)
Run 4	3	3.1624	0.0296	(3.0024, 3.3223)
Run 5	3	3.1468	0.0756	(2.9869, 3.3068)
Run 6	3	3.0682	0.1098	(2.9082, 3.2281)
Run 7	3	2.983	0.188	(2.823, 3.143)

Intensity

The maximum intensity values for UV-C were 6.62 mW/cm^2 after 60 s of exposure at the surface of the emitter for no warm-up time, and 7.98 mW/cm^2 after 60 s of exposure with a 5 min warm-up time (Figure 20). Intensities measured 5, 10, and 15 cm from the emitter decreased as distance increased.

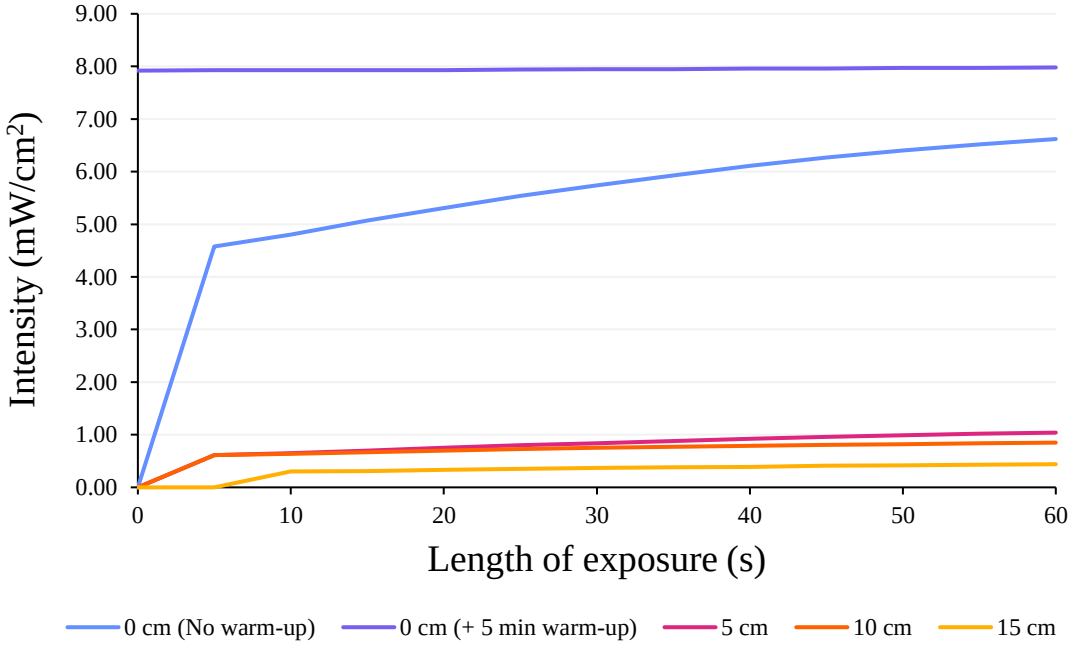

Figure 20: UV-C intensity data at the center of a coupon surface with varying distances from the emitter (λ = 254 nm)

At close distances to the emitter (5 cm), the UV-C intensity varied at separate locations on the #304 stainless steel coupon. Intensity measured at the edge of the coupon was shown to be approximately 0.20 mW/cm^2 lower than at the center (Figure 21). This effect was minimized at further distances (10 and 15 cm).

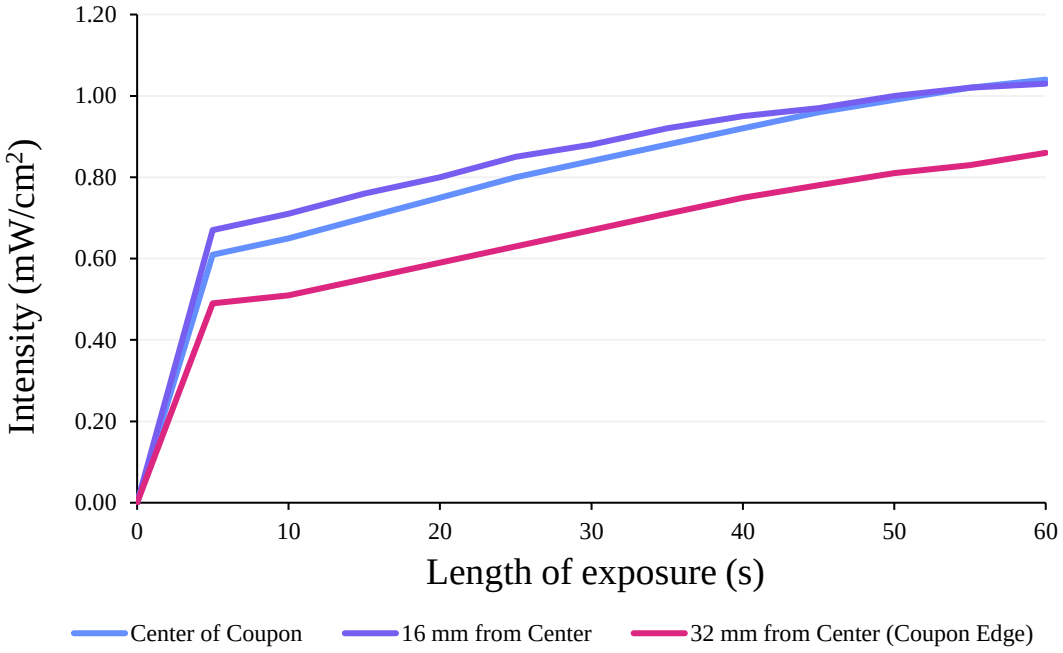

Figure 21: UV-C intensity data at separate locations on coupon surface, 5 cm from emitter (λ = 254 nm)

The maximum intensity values for Far UV-C were 10.13 mW/cm^2 after 60 s of exposure at the surface of the emitter for no "warm-up" time, and 11.72 mW/cm^2 after 60 s of exposure with a 5 min "warm-up" time (Figure 22). Intensities measured 5, 10, and 15 cm from the emitter decreased as distance increased. Because the UV-C and Far UV-C intensity values plateaued under 60 s for each specified distance (5, 10, 15 cm), the maximum intensity value achieved at the end of recording per specified UV device (60 s, Figures 20 & 22) was referenced for dosage modeling.

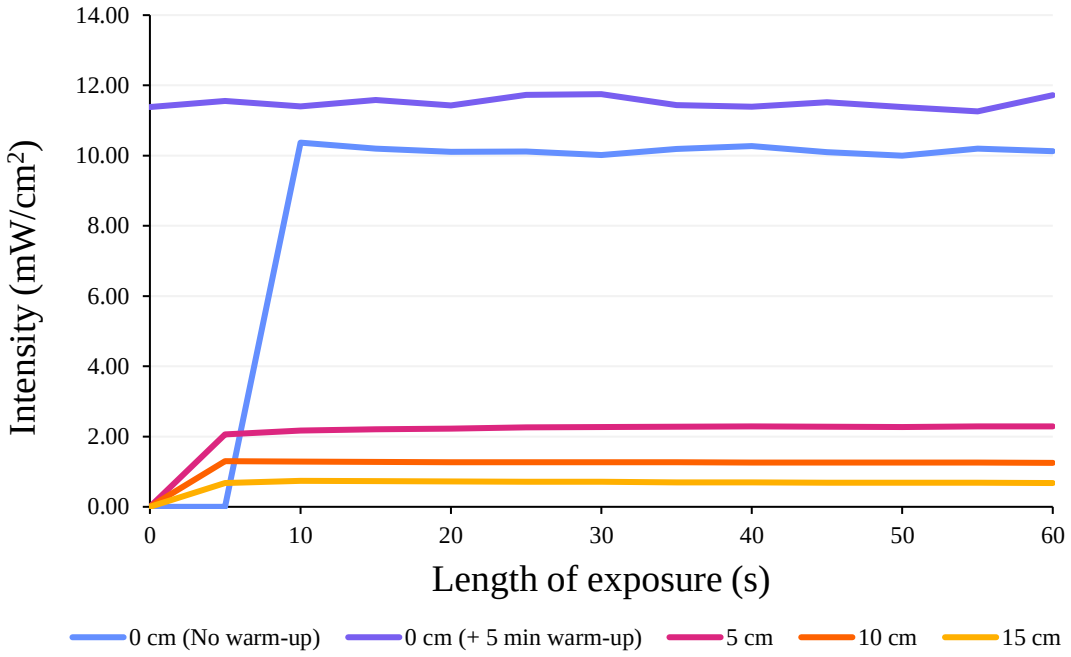

Figure 22: Far UV-C intensity data at the center of a coupon surface with varying distances from the emitter (λ = 222 nm)

The intensity of IR at 0 cm from the emitter was not recorded due to fire hazard. The maximum intensity of IR radiation 5 cm from the emitter was 0.22 mW/cm^2 after 60 min of exposure (Figure 23). Intensities measured 5, 10, and 15 cm from the emitter decreased as distance increased. Because the IR temperature profile did not plateau until approximately 30 min of recording, the intensity values at each specified distance were selected at the measured lengths of exposure for sanitation efficacy data (1, 5, 10, 20 and 60 min) for use in dosage model calculations.

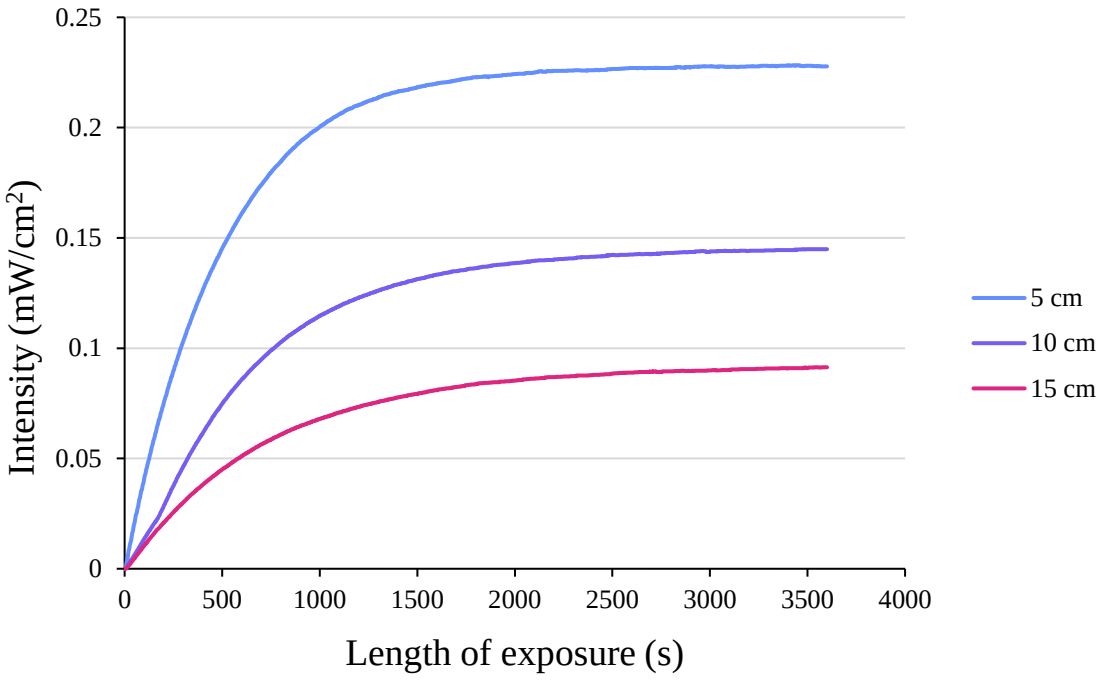

Figure 23: IR intensity data at the center of a coupon surface with varying distances from the emitter

The measured intensity values were consistently lower than the theoretical intensity values calculated using the inverse square law for each technology and distance (Table 4). The largest discrepancy was observed between the theoretical and experimental IR intensity values.

Table 4: Maximum intensity values at specified distances from the emitter

Technology	Maximum Intensity Values (mW/cm^2)					
	5 cm		10 cm		15 cm	
	Experimental	Theoretical	Experimental	Theoretical	Experimental	Theoretical
UV-C	1.04	19.10	0.85	4.77	0.44	2.12
Far UV-C	2.29	127.32	1.25	31.83	0.68	14.15
IR	0.16	1591.55	0.10	397.89	0.06	176.84

Application of UV-C, Far UV-C, and IR Radiation

Both time and intensity were varied to capture a diverse range of radiation exposure dosages. A 3 log reduction in *Salmonella* populations at the maximum intensity was targeted for each sanitation technology.

UV-C reached an average 3.41 ± 0.12 log reduction (mean ± SD, log CFU/cm^2) after 20 min of exposure at 1.04 mW/ cm^2. Figure 24 displays the range of data collected for sanitation efficacy at varying exposure times and intensity values for UV-C radiation.

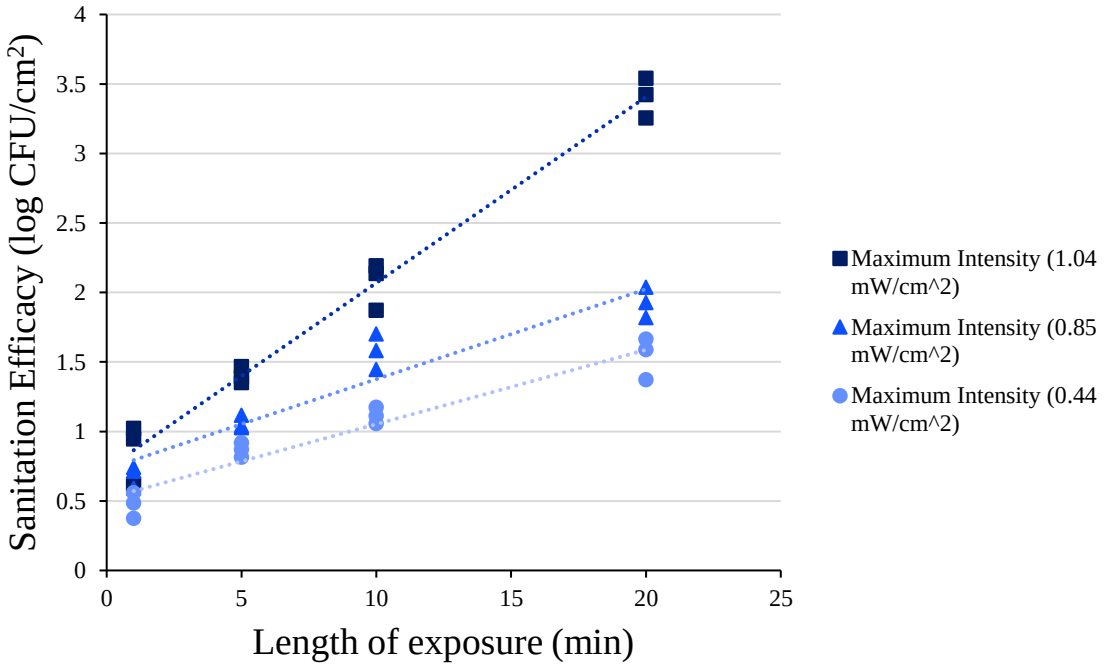

Figure 24: UV-C Salmonella sanitation efficacy (log CFU/cm^2) vs. length of exposure (min) at specified intensities

Far UV-C reached an average 1.68 ± 0.07 log reduction after 10 min of exposure at 2.29 mW/cm^2. Figure 25 displays the range of data collected for sanitation efficacy at varying exposure times and intensity values for Far UV-C radiation. However, the full data was not acquired due to the unexpected failure of the Far UV-C device.

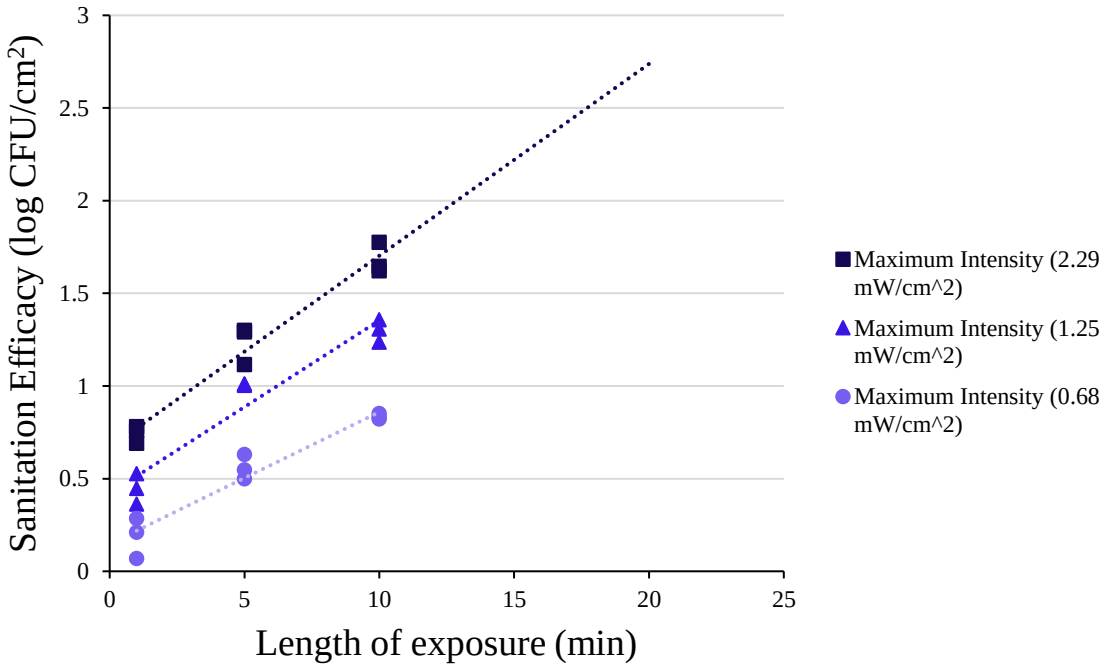

Figure 25: Far UV-C Salmonella sanitation efficacy (log CFU/cm^2) vs. length of exposure (min) at specified intensities

IR reached an average 2.98 ± 0.09 log reduction after 60 min of exposure at 0.23 mW/ cm^2 from the emitter. Figure 26 displays the range of data collected for sanitation efficacy at varying exposure times and intensity values for IR radiation.

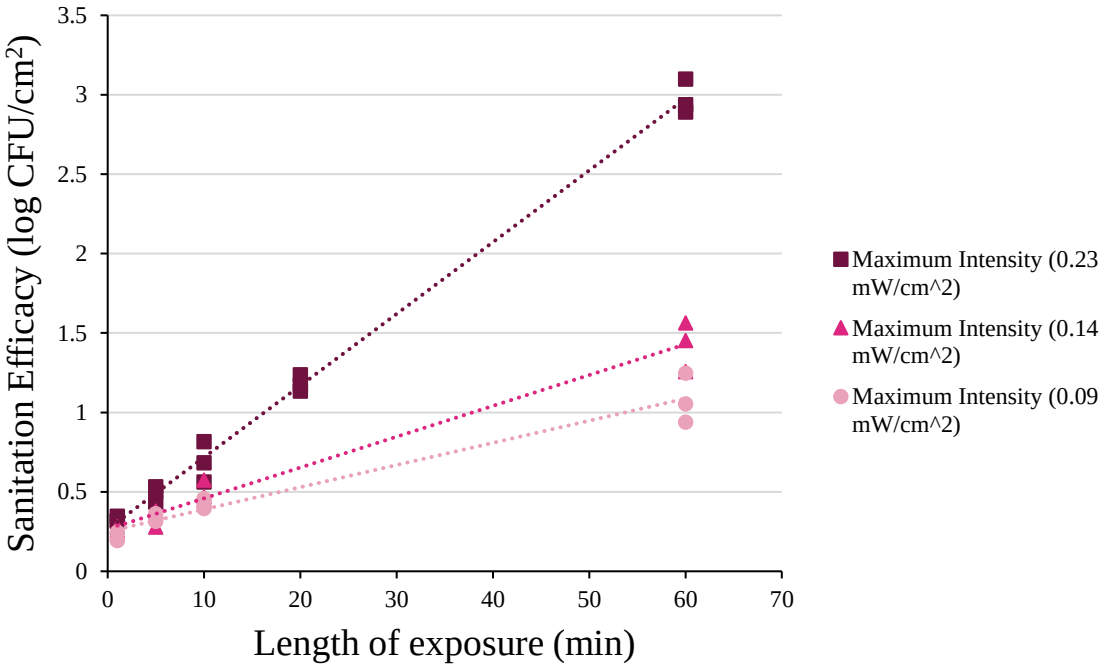

Figure 26: IR Salmonella sanitation efficacy (log CFU/cm^2) vs. length of exposure (min) at specified intensities

Due to the high amount of heat emitted by the IR device, relative humidity fluctuated throughout the treatment. Relative humidity and ambient temperature changed in the sanitation equilibration chamber (initially set to a_w ~0.45) during a 60 min treatment (Table 5).

Table 5: Relative humidity changes during infrared radiation treatment

Time (min)	Relative Humidity (%)	Ambient Chamber Temperature (°C)
0	41.3	20.2
10	37.4	25.4
20	33.9	28.7
30	29.5	28.0
40	27.0	30.1
50	25.4	30.0
60	24.7	32.3

Dosage

The relationship between *Salmonella* reduction and dosage applied to the #304 SS brushed finish coupons for all three sanitation technologies was expressed with individual linear regression analyses and ANCOVA. The regression equations for UV-C, Far UV-C, and IR are featured in equations 4–6.

$$\log\left(\frac{N_0}{N}\right) = 0.6074 + 0.11555 \times \text{UV-C Dosage (mJ/cm}^2\text{)} \quad (4)$$

$$\log\left(\frac{N_0}{N}\right) = 0.4272 + 0.06147 \times \textit{Far UV-C Dosage (mJ/cm}^2\text{)} \quad (5)$$

$$\log\left(\frac{N_0}{N}\right) = 0.3029 + 0.17579 \times \textit{IR Dosage (mJ/cm}^2\text{)} \quad (6)$$

A high percentage of the variation in the reduction could be explained by the models, with R^2 values of 87.90, 86.82, and 94.48% for UV-C, Far UV-C, and IR respectively. Additionally, the RMSE for UV-C, Far UV-C, and IR models were 0.27, 0.17, and 0.18, respectively indicating a good model fit. The linear regression predicted constant coefficients significantly greater than 0 for each model ($p<0.001$). ANCOVA revealed that the interaction between dosage and sanitation technology was significant ($p<0.001$), indicating that the rate of reduction was significantly different between technologies. IR radiation displayed the highest reduction rate, followed by UV-C and Far UV-C (Figure 27).

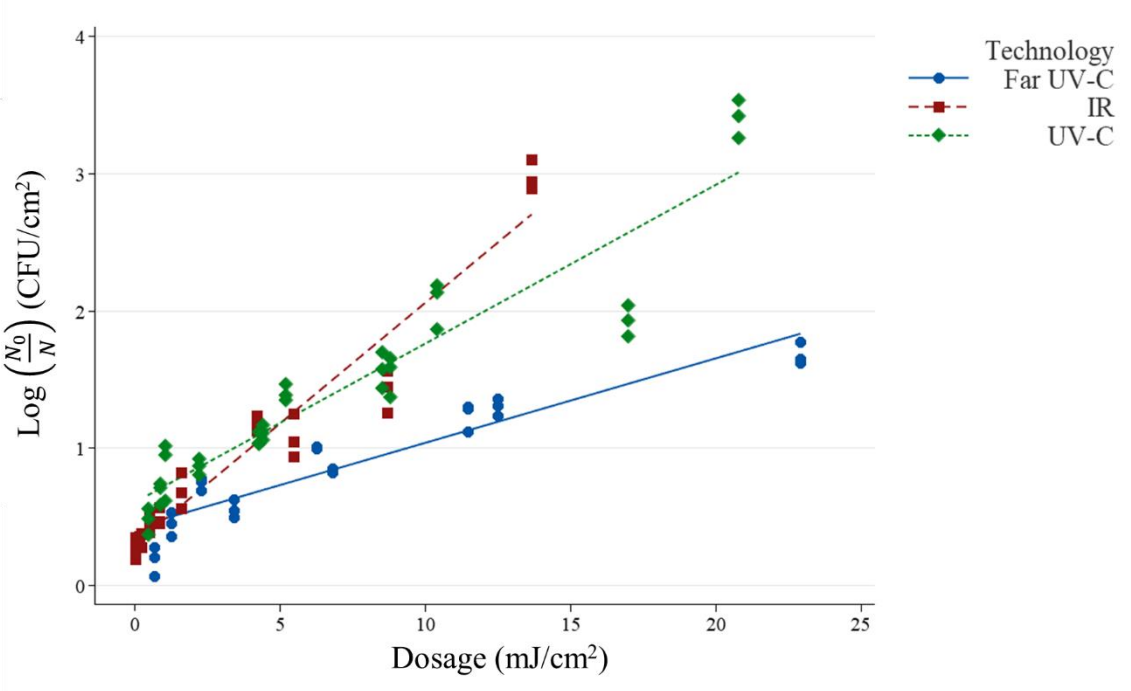

Figure 27: Sanitation efficacy (log CFU/cm^2) vs. dosage (mJ/cm^2)

The predicted reduction rate parameters from the linear regression were used to calculate the range of dosages predicted to achieve a target reduction value 95% of the time. Predicted intercept parameters were not included in the calculations to provide a more conservative dosage estimate. Target reduction values ranged from 1 to 5 log reductions (Table 6).

Table 6: 95% Confidence intervals of the required dosage to meet a target sanitation efficacy (log CFU/cm^2)

Sanitation Efficacy (reduction)	IR Dosage	UV-C Dosage	Far UV-C Dosage
log CFU/cm^2	mJ/cm^2	mJ/cm^2	mJ/cm^2
1	(5.26, 6.19)	(7.66, 9.94)	(14.02, 19.38)
2	(10.53, 12.37)	(15.33, 19.88)	(28.03, 38.75)
3	(15.79, 18.56)	(22.99, 29.82)	(42.05, 58.13)

Discussion

The electrostatic powder coating dry inoculation method achieved higher than 5 log CFU/cm^2 on the surface of stainless steel coupons on coated coupons. In comparison to other studies, the biofilm method from De Oliviera (2010) adhered 4.89 ± 0.03 log CFU/cm^2 onto #304 SS. Powder coated #304 SS coupons in this study achieved 5.45 ± 0.59 log CFU/cm^2. The milk powder transfer method by Chen & Snyder (2023) adhered 3.3 ± 0.2 log CFU/coupon and had 1.2 ± 0.4 log CFU/coupon of *Salmonella* populations remaining on #304 SS after cleaning. In comparison, the average populations on visibly cleaned coupons for the sanitation portion of this experiment were 3.09 ± 0.16 log CFU/cm^2. With similar resultant populations in comparison to other studies, the powder coating method is a promising dry inoculation methodology for cleaning and sanitation studies.

The powder coating methodology has several advantages in comparison to other food contact surface inoculation strategies. First, the inoculation method does not use liquid broths to adhere microorganisms to the target surface, minimizing the amount of moisture introduced into the experimental environment. Secondly, this method does not rely on biofilm formation or glass beads to transfer and inoculate target surfaces with microorganisms. Because of this, the method can directly simulate *Salmonella* contamination from the food product itself to relevant equipment surfaces instead of using an unrelated intermediate in the process. Lastly, the method does not require mechanical actions such as mixing the target surfaces in a sealed container to accrue inoculated powders on the target surface. Instead, the inoculated powder is adhered through electrostatic charge, which replicates dust accrual on surfaces generated by equipment during operation. Incidentally, the inoculated wheat berry grinding process used in this study displayed this phenomenon of dust accrual on the surface of an aluminum grain milling

attachment without the use of an electrostatic powder coating gun (Figure 1). Comparisons of microorganism populations between surfaces inoculated using the electrostatic coating gun and the triboelectrically-charged powder generated by milling equipment are another potential avenue for determining an ideal dry powder inoculation strategy.

Of the selected technologies, IR had the highest log reduction per dosage (Figure 27), followed by UV-C and Far UV-C. However, relying solely on the dosage metric for technology decisions can be deceptive. Despite having the highest reduction per dosage, the length of exposure (~60 min) needed to achieve a 3 log reduction for IR at its highest measured intensity was over twice that needed for UV-C (~20 min) or Far UV-C (~25). This is because the measured intensity of the IR was appreciably lower than the UV technologies (Table 5). This highlights the importance of understanding the time needed to achieve a given dosage for each technology. Of the technologies and radiation intensities available for use in this study, none were able to achieve > 3 log reduction in populations within short exposure times (< 5 mins). As it currently stands, the long time required for radiative sanitation technologies to achieve appreciable amounts of kill on equipment surfaces limits its uses within a food processing environment.

The log reduction per dosage for UV-C was significantly greater than Far UV-C. This indicates that the 254 nm wavelength was more efficient in inactivating *Salmonella* in comparison to 222 nm. This agrees with the conclusions reported by Hessling, et al., which discussed the phenomena of 254 nm wavelengths having a higher relative absorption by DNA and proteins compared to 222 nm (Hessling et al., 2021). However, further considerations towards human health and safety must be made when selecting UV-C wavelength. The 222 nm wavelength has been shown to be less harmful to ocular membranes and skin in comparison to

the 254 nm wavelength (Napoleão et al., 2023). Therefore, UV-C should be prioritized in situations where human exposure is minimized, such as within enclosed spaces, the inside of equipment, planar surfaces, and the underside of conveyor belts. Far UV-C has potential applications for areas where sanitation personnel may be present during the cleaning and sanitation process or in open spaces.

IR technologies may be a viable solution for inaccessible areas in conductive equipment. IR can penetrate through surfaces while UV-C cannot. However, elevated temperatures during experimentation revealed an important consideration in the use of IR radiation in low moisture processing environments. The IR device reached a maximum temperature of 153.6°C at 5 cm from the emitter after 57 min of exposure. A major safety consideration in low-moisture food processing environments with IR is the risk of dust explosions. Dust explosions can occur from five factors (known as the dust explosion pentagon): oxygen, heat, fuel, dispersion, and confinement (Occupational Safety and Health Administration, 2015). If a heat source is added to an environment with airborne particles, the risk of dust explosion can increase. Therefore, IR surfaces should be separated from dusty surfaces and used sparingly, only for hard-to-reach nooks and crannies where UV-C cannot penetrate, such as between tightened nuts, bolts, and washers on equipment.

The theoretical and experimentally retrieved intensity values for each technology were different than expected. In particular, the discrepancies between the theoretical and experimentally achieved IR intensity values (Table 5) may be due to the assumption that all 500 W of energy from the emitter was being applied to the target surface as a point. In reality, the radiation was emitted in a top down (linear) fashion. Additional calculations to determine the view factor of emitted radiation from the rectangular ports in the sanitation equilibration

chamber (Figure 9) and the circular surface of the coupon may improve the accuracy of the theoretically calculated intensities. Factors such as the emissivity of the radiating surfaces, the absorptivity of the coupon, and any intervening medium's impact on radiation propagation should also be considered. Additionally, refining the view factor calculations to account for geometric alignments and surface orientations can further enhance the predictive accuracy regarding radiation heat transfer. The IR passed through an optically clear temperature-resistant piece of glass that prevented the sanitation equilibration chamber top from melting under the intense heat of the IR emitter, which may have impacted the IR emitted to the target surface. Additionally, as evidenced in Figure 23, the intensity varied on the surface of the coupon depending on the location of the UV-C light sensor. Miniscule adjustments to the intensity measurement set up (Figure 14) may have impacted the recorded intensity values for each technology.

Importantly, the application of the dosage models and suggestions are dependent on environmental factors and the nature of the processing line. One technology does not fit all low moisture food processing situations. These technologies are beneficial for closed systems and spot treatments, especially as a “passive” form of sanitation that requires minimal labor from personnel. Radiative sanitation technologies are additional tools to increase the amount of hurdles for microorganism survival and cross-contamination in dry processing environments.

CONCLUSIONS

Objective 1: Develop Replicable and Consistent Electrostatic Powder Coating Dry Inoculation Methodology

- The dry electrostatic powder coating methodology consistently and reliably adhered inoculated, custom fabricated flour to the surface of #304 brushed finish, #304 mirror finish, and #316L brushed finish coupons. The inoculation method adhered greater than an average 5 log CFU/cm^2 of *Salmonella* populations to the surface of #304 brushed finish and #316L brushed finish SS coupons. Visibly cleaned coupons achieved ~4 log CFU/cm^2 on the surface of #304 brushed finish and #316L brushed finish SS coupons.
- Stainless steel finish and grade did not significantly impact the *Salmonella* populations adhered using the dry powder coating methodology.
- The consistency and replicability of the inoculation methodology had mixed success. The initial visibly cleaned population counts used in the sanitation portion of the experiment were lower than those achieved in the evaluation of the powder coating methodology portion on #304 SS (3.09 ± 0.16 log CFU/cm^2 vs. the initial 3.92 ± 0.57 log CFU/cm^2). However, there were no significant differences between the average visibly cleaned populations between sanitation experimental runs. The largest standard deviation observed for a sanitation run was 0.17 log CFU/cm^2 (Table 3). This showed that the inoculation method was both consistent and replicable with minimized variability within a single run.

Objective 2: Evaluate Performance of Non-Aqueous Sanitation Technologies

- Two of the radiative technologies used in this study (UV-C and IR) achieved a sanitation efficacy of > 3 log CFU/cm^2 on the surface of #304 brushed finish coupons. Far UV-C did not achieve this target due to equipment malfunction.

- UV-C 254 nm had the highest sanitation efficacy with the shortest length of exposure, followed by Far UV-C and IR.

Objective 3: Generate A Descriptive Model for *Salmonella* Population Reductions on Stainless Steel Surfaces

- Three individual linear regression models were developed to describe the dosages obtained experimentally on SS surfaces.
- The dosage required to achieve a target sanitation efficacy (log reduction) was calculated using the 95% confidence intervals generated from the ANCOVA of the linear regression models.
- Suggestions were provided for the implementation of each radiative technology.

Future Work

- This study kept the relative humidity in the powder coating chamber and sanitation chamber constant with a target value of 45%. More research is needed to characterize the impact of relative humidity toward the efficacy of non-aqueous sanitation technologies.
- The wheat berry milling process generated a fine layer of inoculated dust on the surface of the milling attachment without the use of an electrostatic powder coating gun. The utilization of triboelectric charge in inoculated powders should be explored as an alternative dry inoculation method for food contact surfaces.
- This study focused on stainless steel food contact surfaces for inoculation due to their ubiquity and electrical conductivity. The electrostatic powder coating method should be explored with other electrically grounded food contact materials, such as HDPE, in low-moisture food production environments.

- The intensity in this experiment was modulated by increasing the distance between the target surface and the radiation emitter. Further research into high intensity devices will also be beneficial.
- Further investigation into the synergistic effects of UV-C and IR radiation on contaminated surfaces may reduce the exposure time required for targeted sanitation efficacies.

BIBLIOGRAPHY

Alonso, V. P. P., Goncalves, M., de Brito, F. A. E., Barboza, G. R., Rocha, L. D., & Silva, N. C. C. (2023). Dry surface biofilms in the food processing industry: An overview on surface characteristics, adhesion and biofilm formation, detection of biofilms, and dry sanitization methods. *Comprehensive Reviews in Food Science and Food Safety*, *22*(1), 688-713. https://doi.org/10.1111/1541-4337.13089

Bae, Y. M., & Lee, S. Y. (2012). Inhibitory effects of UV treatment and a combination of UV and dry heat against pathogens on stainless steel and polypropylene surfaces. *Journal of Food Science*, *77*(1), M61-M64. https://doi.org/10.1111/j.1750-3841.2011.02476.x

Bailey, A. G. (1998). The science and technology of electrostatic powder spraying, transport and coating. *Journal of Electrostatics*, *45*(2), 85-120. https://doi.org/10.1016/s0304-3886(98)00049-7

Batista, L. F. Z., Kaina, B., Meneghini, R., & Menck, C. F. M. (2009). How DNA lesions are turned into powerful killing structures: Insights from UV-induced apoptosis. *Mutation Research-Reviews in Mutation Research*, *681*(2-3), 197-208. https://doi.org/10.1016/j.mrrev.2008.09.001

Beck, S. E., Rodriguez, R. A., Hawkins, M. A., Hargy, T. M., Larason, T. C., & Linden, K. G. (2016). Comparison of UV-induced inactivation and RNA damage in MS2 phage across the germicidal UV spectrum. *Applied and Environmental Microbiology*, *82*(5), 1468-1474. https://doi.org/10.1128/aem.02773-15

Bennett, J. E. (2020). *Mandell, Douglas, and Bennett's Principles and Practice of Infectious Diseases: 2-Volume Set* (D. Raphael & J. B. Martin, Eds. 9 ed.). Elsevier.

Berghofer, L. K., Hocking, A. D., Miskelly, D., & Jansson, E. (2003). Microbiology of wheat and flour milling in Australia. *International Journal of Food Microbiology*, *85*(1-2), 137-149. https://doi.org/10.1016/s0168-1605(02)00507-x

Bolton, J. R., & Linden, K. G. (2003). Standardization of methods for fluence (UV dose) determination in bench-scale UV experiments. *Journal of Environmental Engineering*, *129*(3), 209-215. https://doi.org/doi:10.1061/(ASCE)0733-9372(2003)129:3(209)

Bozkurt, T., & Uslu, F. M. (2022). Inactivation effect of ultraviolet-C (UVC) irradiation on different microorganisms: Staphylococcus aureus, Bacillus cereus, Escherichia coli and Klebsiella pneumoniae. *Acta Microbiologica Hellenica*, *67*(1), 39-48.

Buonanno, M., Ponnaiya, B., Welch, D., Stanislauskas, M., Randers-Pehrson, G., Smilenov, L., . . . Brenner, D. J. (2017). Germicidal efficacy and mammalian skin safety of 222-nm UV light. *Radiation Research*, *187*(4), 483-491. https://doi.org/10.1667/rr0010cc.1

Carter, B. P., Galloway, M. T., Morris, C. F., Weaver, G. L., & Carter, A. H. (2015). The case for water activity as a specification for wheat tempering and flour production. *Cereal Foods World*, *60*(4), 166-170. https://doi.org/10.1094/cfw-60-4-0166

CDC Yellow Book. (2024a). *Salmonellosis, Nontyphoidal.* Centers for Disease Control and Prevention. https://wwwnc.cdc.gov/travel/yellowbook/2024/infections-diseases/salmonellosis-nontyphoidal

CDC Yellow Book. (2024b). *Typhoid & Paratyphoid Fever*. Centers for Disease Control and Prevention. https://wwwnc.cdc.gov/travel/yellowbook/2024/infections-diseases/typhoid-and-paratyphoid-fever

Centers for Disease Control and Prevention. (1998). *Multistate Outbreak of Salmonella Serotype Agona Infections Linked to Toasted Oats Cereal—United States, April–May, 1998*. M. a. M. W. Report.

Centers for Disease Control and Prevention. (2004). *Outbreak of Salmonella Serotype Enteritidis Infections Associated with Raw Almonds—United States and Canada, 2003– 2004*. M. a. M. W. R. Dispatch. https://www.cdc.gov/mmwr/preview/mmwrhtml/mm53d604a1.htm

Centers for Disease Control and Prevention. (2007). *Multistate outbreak of Salmonella serotype Tennessee infections associated with peanut butter—United States, 2006–2007*. https://www.cdc.gov/mmwr/preview/mmwrhtml/mm5621a1.htm

Centers for Disease Control and Prevention. (2008). *Multistate Outbreak of Salmonella Agona Infections Linked to Rice and Wheat Puff Cereal (FINAL UPDATE)*. https://www.cdc.gov/salmonella/2008/rice-wheat-puff-cereal-5-13-2008.html

Centers for Disease Control and Prevention. (2010). *Salmonella Montevideo Infections Associated with Salami Products Made with Contaminated Imported Black and Red Pepper—United States, July 2009–April 2010*. M. a. M. W. Report. https://www.cdc.gov/mmwr/preview/mmwrhtml/mm5950a3.htm

Centers for Disease Control and Prevention. (2013). *Multistate outbreak of Salmonella Montevideo and Salmonella Mbandaka infections linked to tahini sesame paste (Final Update) 2013*. M. a. M. W. Report.

Centers for Disease Control and Prevention. (2016). *National Enteric Disease Surveillance: Salmonella Annual Report, 2016*. https://www.cdc.gov/nationalsurveillance/pdfs/2016-Salmonella-report-508.pdf

Centers for Disease Control and Prevention. (2023a). *Salmonella Outbreak Linked to Flour*. Retrieved 30 March from https://www.cdc.gov/salmonella/infantis-03-23/details.html

Centers for Disease Control and Prevention. (2023b). *Salmonella Outbreak Linked to Raw Cookie Dough*. Retrieved 30 March from https://www.cdc.gov/salmonella/Enteritidis-05-23/index.html

Cereal flours and related products, 21 C.F.R. § 137.105 (2024). https://www.ecfr.gov/current/title-21/chapter-I/subchapter-B/part-137

Chen, L., & Snyder, A. B. (2023). Surface inoculation method impacts microbial reduction and transfer of *Salmonella* Enteritidis PT 30 and potential surrogates during dry sanitation. *Int J Food Microbiol*, *406*, 110405. https://doi.org/10.1016/j.ijfoodmicro.2023.110405

de Oliveira, M. M. M., Brugnera, D. F., Alves, E., & Piccoli, R. H. (2010). Biofilm formation by *Listeria monocytogenes* on stainless steel surface and biotransfer potential. *Brazilian Journal of Microbiology*, *41*(1), 97-106. https://doi.org/10.1590/s1517-83822010000100016

Daeschel, D., Rana, Y. S., Chen, L., Cai, S. Y., Dando, R., & Snyder, A. B. (2023). Visual inspection of surface sanitation: Defining the conditions that enhance the human threshold for detection of food residues. *Food Control*, *149*, Article 109691. https://doi.org/10.1016/j.foodcont.2023.109691

Demeersseman, N., Saegeman, V., Devriese, H., & Schuermans, A. (2023). Shedding a light on ultraviolet-C technologies in the hospital environment. *Journal of Hospital Infection*, *132*, 85-92. https://doi.org/10.1016/j.jhin.2022.12.009

Du, W.-X., Danyluk, M. D., & Harris, L. J. (2010). Efficacy of aqueous and alcohol-based quaternary ammonium sanitizers for reducing *Salmonella* in dusts generated in almond hulling and shelling facilities. *Journal of Food Science*, *75*(1), M7-M13. https://doi.org/10.1111/j.1750-3841.2009.01393.x

El Darra, N., Xie, F., Kamble, P., Khan, Z., & Watson, I. (2021). Decontamination of *Escherichia coli* on dried onion flakes and black pepper using infra-red, ultraviolet and ozone hurdle technologies. *Heliyon*, *7*(6), Article e07259. https://doi.org/10.1016/j.heliyon.2021.e07259

Fedrizzi, L., Stenico, M., Deflorian, F., Maschio, S., & Bonora, P. L. (2007). Effect of powder painting procedures on the filiform corrosion of aluminium profiles. *Progress in Organic Coatings*, *59*(3), 230-238. https://doi.org/10.1016/j.porgcoat.2006.02.011

Gabriel, A. A., Ballesteros, M. L. P., Rosario, L. M. D., Tumlos, R. B., & Ramos, H. J. (2018). Elimination of *Salmonella* enterica on common stainless steel food contact surfaces using UV-C and atmospheric pressure plasma jet. *Food Control*, *86*, 90-100. https://doi.org/10.1016/j.foodcont.2017.11.011

Ghori, M. U., Supuk, E., & Conway, B. R. (2015). Tribo-electrification and powder adhesion studies in the development of polymeric hydrophilic drug matrices. *Materials*, *8*(4), 1482-1498. https://doi.org/10.3390/ma8041482

Giese, N., & Darby, J. (2000). Sensitivity of microorganisms to different wavelengths of UV light: Implications on modeling of medium pressure UV systems. *Water Research*, *34*(16), 4007-4013. https://doi.org/10.1016/s0043-1354(00)00172-x

Goodsell, D. S. (2001). The molecular perspective: Ultraviolet light and pyrimidine dimers. *Oncologist*, *6*(3), 298-299. https://doi.org/10.1634/theoncologist.6-3-298

Ha, J. W., & Kang, D. H. (2013). Simultaneous near-infrared radiant heating and UV radiation for inactivating *Escherichia coli* O157:H7 and *Salmonella* enterica serovar typhimurium in powdered red pepper (capsicum annuum l.). *Applied and Environmental Microbiology*, *79*(21), 6568-6575. https://doi.org/10.1128/aem.02249-13

Hamanaka, D., Norimura, N., Baba, N., Mano, K., Kakiuchi, M., Tanaka, F., & Uchino, T. (2011). Surface decontamination of fig fruit by combination of infrared radiation heating with ultraviolet irradiation. *Food Control*, *22*(3-4), 375-380. https://doi.org/10.1016/j.foodcont.2010.09.005

Harada, A. M. M., & Nascimento, M. S. (2021). Efficacy of dry sanitizing methods on Listeria monocytogenes biofilms. *Food Control*, *124*, Article 107897. https://doi.org/10.1016/j.foodcont.2021.107897

Hessling, M., Haag, R., Sieber, N., & Vatter, P. (2021). The impact of far-UVC radiation (200-230 nm) on pathogens, cells, skin, and eyes - a collection and analysis of a hundred years of data. *Gms Hygiene and Infection Control*, *16*, Article Doc07. https://doi.org/10.3205/dgkh000378

Hildebrandt, I. M., Marks, B. P., Ryser, E. T., Villa-Rojas, R., Tang, J., Garces-Vega, F. J., & Buchholz, S. E. (2016). Effects of inoculation procedures on variability and repeatability

of Salmonella thermal resistance in wheat flour. *Journal of Food Protection*, *79*(11), 1833-1839.

International Organization for Standardization. (2007). Space environment (natural and artificial)— Process for determining solar irradiances. In *ISO 21348* (pp. 1-12).

Kaidzu, S., Sugihara, K., Sasaki, M., Nishiaki, A., Ohashi, H., Igarashi, T., & Tanito, M. (2022). Safety evaluation of far UV-C irradiation to epithelial basal cells in the corneal limbus. *Photochemistry and Photobiology*. https://doi.org/10.1111/php.13750

Kane, D. M., Getty, K. J. K., Mayer, B., & Mazzotta, A. (2016). Sanitizing in dry-processing environments using isopropyl alcohol quaternary ammonium formula. *Journal of Food Protection*, *79*(1), 112-116. https://doi.org/10.4315/0362-028x.jfp-15-257

Kim, S.-J., Kim, D.-K., & Kang, D.-H. (2016). Using UVC light-emitting diodes at wavelengths of 266 to 279 nanometers to inactivate foodborne pathogens and pasteurize sliced cheese. *Applied and Environmental Microbiology*, *82*(1), 11-17. https://doi.org/10.1128/aem.02092-15

Kim, Y.-J., Lee, J.-I., & Kang, D.-H. (2023). Simultaneous vacuum ultra violet-amalgam lamp radiation and near-infrared radiation heating for a synergistic bactericidal effect against *Escherichia coli* O157:H7 and *Salmonella* enterica serovar Typhimurium in black peppercorn. *Food Research International*, *169*, Article 112827. https://doi.org/10.1016/j.foodres.2023.112827

Kusumaningrum, H. D., Riboldi, G., Hazeleger, W. C., & Beumer, R. R. (2003). Survival of foodborne pathogens on stainless steel surfaces and cross-contamination to foods. *International Journal of Food Microbiology*, *85*(3), 227-236. https://doi.org/10.1016/s0168-1605(02)00540-8

Lin, Y. W., Simsek, S., & Bergholz, T. M. (2023). Fate of *Salmonella* and shiga-toxin producing *Escherichia coli* on wheat grain during tempering. *Food Microbiology*, *111*, Article 104194. https://doi.org/10.1016/j.fm.2022.104194

Liu, S. M., Keller, S. E., & Anderson, N. M. (2022). Transfer of *Salmonella* from inert food contact surfaces to wheat flour, cornmeal, and NaCl. *Journal of Food Protection*, *85*(2), 231-237. https://doi.org/10.4315/jfp-21-225

Liu, S. X., Tang, J. M., Tadapaneni, R. K., Yang, R., & Zhu, M. J. (2018). Exponentially increased thermal resistance of *Salmonella* spp. and *Enterococcus faecium* at reduced water activity. *Applied and Environmental Microbiology*, *84*(8), Article e02742-17. https://doi.org/10.1128/aem.02742-17

McCallum, L., Paine, S., Sexton, K., Dufour, M., Dyet, K., Wilson, M., . . . Hope, V. (2013). An outbreak of *Salmonella* typhimurium phage type 42 associated with the consumption of raw flour. *Foodborne Pathogens and Disease*, *10*(2), 159-164. https://doi.org/10.1089/fpd.2012.1282

Moretro, T., Martens, L., Teixeira, P., Ferreira, V. B., Maia, R., Maugesten, T., & Langsrud, S. (2020). Is visual motivation for cleaning surfaces in the kitchen consistent with a hygienically clean environment? *Food Control*, *111*, Article 107077. https://doi.org/10.1016/j.foodcont.2019.107077

Myoda, S. P., Gilbreth, S., Akins-Leventhal, D., Davidson, S. K., & Samadpour, M. (2019). Occurrence and levels of *Salmonella*, enterohemorrhagic *Escherichia coli*, and *Listeria* in raw wheat. *Journal of Food Protection*, *82*(6), 1022-1027. https://doi.org/10.4315/0362-028x.jfp-18-345

Napoleão, R. S., Adamoski, D., Girasole, A., Lima, E. N., Justo-Junior, A. D., Domingues, R., . . . Dias, S. M. G. (2023). Different biological effects of exposure to far-UVC (222 nm) and near-UVC (254 nm) irradiation. *Journal of Photochemistry and Photobiology B-Biology*, *243*, Article 112713. https://doi.org/10.1016/j.jphotobiol.2023.112713

Navarathna, T., Jinadatha, C., Corona, B. A., Coppin, J. D., Choi, H., Bennett, M. R., . . . Chatterjee, P. (2023). Efficacy of a filtered far-UVC handheld disinfection device in reducing the microbial bioburden of hospital surfaces. *American Journal of Infection Control*, *51*(12), 1406-1410. https://doi.org/10.1016/j.ajic.2023.05.003

Nyhan, L., Przyjalgowski, M., Lewis, L., Begley, M., & Callanan, M. (2021). Investigating the use of ultraviolet light emitting diodes (UV-LEDs) for the inactivation of bacteria in powdered food ingredients. *Foods*, *10*(4), Article 797. https://doi.org/10.3390/foods10040797

Occupational Safety and Health Administration. (2015). Hazard alert: Combustible dust explosions. In *OSHA Fact Sheet*: United States Department of Labor.

Orevi, T., & Kashtan, N. (2021). Life in a droplet: microbial ecology in microscopic surface wetness. *Frontiers in Microbiology*, *12*, Article 655459. https://doi.org/10.3389/fmicb.2021.655459

Pilcher, G. R. (2001). Meeting the challenge of radical change: Coatings R&D as we enter the 21st century. *Journal of Coatings Technology*, *73*(921), 135-+. https://doi.org/10.1007/bf02697998

Posner, E. S., & Hibbs, A. N. (2005). Wheat flour milling. Amer Assn of Cereal Chemists.

Prasad, L. K., McGinity, J. W., & Williams, R. O. (2016). Electrostatic powder coating: Principles and pharmaceutical applications. *International Journal of Pharmaceutics*, *505*(1-2), 289-302. https://doi.org/10.1016/j.ijpharm.2016.04.016

Ramos, C. C. R., Roque, J. L. A., Sarmiento, D. B., Suarez, L. E. G., Sunio, J. T. P., Tabungar, K. I. B., . . . Hilario, A. L. (2020). Use of ultraviolet-C in environmental sterilization in hospitals: A systematic review on efficacy and safety. *International Journal of Health Sciences-Ijhs*, *14*(6), 52-65.

Ruiz-Hernandez, K., Ramirez-Rojas, N. Z., Meza-Plaza, E. F., Garcia-Mosqueda, C., Jauregui-Vazquez, D., Rojas-Laguna, R., & Sosa-Morales, M. E. (2021). UV-C treatments against *Salmonella* Typhimurium ATCC 14028 in inoculated peanuts and almonds. *Food Engineering Reviews*, *13*(3), 706-712. https://doi.org/10.1007/s12393-020-09272-7

Sabillón, L., Stratton, J., Rose, D., & Bianchini, A. (2021). Microbiological survey of equipment and wheat-milled fractions of a milling operation. *Cereal Chemistry*, *98*(1), 44-51. https://doi.org/10.1002/cche.10373

Sabillón, L., Stratton, J., Rose, D. J., Regassa, T. H., & Bianchini, A. (2016). Microbial load of hard red winter wheat produced at three growing environments across Nebraska, USA. *Journal of Food Protection*, *79*(4), 646-654. https://doi.org/10.4315/0362-028x.jfp-15-424

Scallan, E., Hoekstra, R. M., Angulo, F. J., Tauxe, R. V., Widdowson, M. A., Roy, S. L., . . . Griffin, P. M. (2011). Foodborne illness acquired in the United States-major pathogens. *Emerging Infectious Diseases*, *17*(1), 7-15. https://doi.org/10.3201/eid1701.P11101

Sliney, D. (2013). Balancing the risk of eye irritation from UV-C with infection from bioaerosols. *Photochemistry and Photobiology*, *89*(4), 770-776. https://doi.org/10.1111/php.12093

Smith, D. F., Hildebrandt, I., Casulli, K. E., Dolan, K. D., & Marks, B. P. (2016). Modeling the effect of temperature and water activity on the thermal resistance of *Salmonella* Enteritidis PT 30 in wheat flour. Journal of Food Protection, 79(12), 2058–2065. https://doi.org/10.4315/0362-028x.jfp-16-155

Somboonvechakarn, C., & Barringer, S. A. (2012). Effect of particle density and composition on mixtures during nonelectrostatic and electrostatic powder coating. *Journal of Food Process Engineering*, *35*(2), 236-249. https://doi.org/10.1111/j.1745-4530.2010.00585.x

Sperber, W. H., & North American Millers' Association. (2007). Role of microbiological guidelines in the production and commercial use of milled cereal grains: A practical

approach for the 21st century. *Journal of Food Protection*, *70*(4), 1041-1053. https://doi.org/10.4315/0362-028x-70.4.1041

Suehr, Q. J. (2020). *Adhesion Mechanics and Physical Characteristics of Salmonella Enteritidis in Low Moisture Environments* [Masters thesis, Michigan State University]. ProQuest.

Syamaladevi, R. M., Tadapaneni, R. K., Xu, J., Villa-Rojas, R., Tang, J., Carter, B., . . . Marks, B. (2016). Water activity change at elevated temperatures and thermal resistance of *Salmonella* in all purpose wheat flour and peanut butter. *Food Research International*, *81*, 163-170.

Villa-Rojas, R., Zhu, M.-J., Paul, N. C., Gray, P., Xu, J., Shah, D. H., & Tang, J. (2017). Biofilm forming *Salmonella* strains exhibit enhanced thermal resistance in wheat flour. *Food Control*, *73*, 689-695.

Wei, X. Y., Lau, S. K., Chaves, B. D., Danao, M. G. C., Agarwal, S., & Subbiah, J. (2020). Effect of water activity on the thermal inactivation kinetics of *Salmonella* in milk powders. *Journal of Dairy Science*, *103*(8), 6904-6917. https://doi.org/10.3168/jds.2020-18298

Xu, J., Shah, D., Song, J., & Tang, J. (2020). Changes in cellular structure of heat-treated *Salmonella* in low-moisture environments. *Journal of Applied Microbiology*, *129*(2), 434-442.

Xu, J., Tang, J., Jin, Y., Song, J., Yang, R., Sablani, S. S., & Zhu, M.-J. (2019). High temperature water activity as a key factor influencing survival of *Salmonella* Enteritidis PT30 in thermal processing. *Food Control*, *98*, 520-528.

Yoon, J. H., Hyun, J. E., Song, H., Kim, J. Y., Kim, J. H., & Lee, S. Y. (2018). Food residuals on the food-contacting surfaces of stainless steel and polypropylene influence the efficacy of ultraviolet light in killing foodborne pathogens. *Journal of Food Safety*, *38*(5), Article e12506. https://doi.org/10.1111/jfs.12506

Zhabinskaya, D. & University of California Davis. (2023a, January 19). 9.2: Particle model of light. Physics LibreTexts. https://phys.libretexts.org/Courses/University_of_California_Davis/UCD:_Physics_7C_-_General_Physics/9:_Quantum_Mechanics/9.2:_Particle_Model_of_Light

Zhabinskaya, D. & University of California Davis. (2023b, January 19). 9.3: Energy quantization. Physics LibreTexts. https://phys.libretexts.org/Courses/University_of_California_Davis/UCD%3A_Physics_7C_-_General_Physics/9%3A_Quantum_Mechanics/9.3%3A_Energy_Quantization